

Synergistic Fat-Reducing Effect of Deoxycholic Acid and Rhein in Lipid-Based Nanoparticles with Reduced Toxicity for Obesity Treatment

Ching-Yun Hsu^{1,2,*}, Tse-Hung Huang^{3,4,5,*}, Zih-Chan Lin⁷, Chih-Jung Chen⁸⁻¹⁰, Erica Hwang¹¹, Wei-Jhang Chen¹², Jia-You Fang^{12,13}

¹Department of Nutrition and Health Sciences, Chang Gung University of Science and Technology, Kweishan, Taoyuan, Taiwan; ²Research Center for Food and Cosmetic Safety and Research Center for Chinese Herbal Medicine, Chang Gung University of Science and Technology, Kweishan, Taoyuan, Taiwan; ³Department of Traditional Chinese Medicine, Chang Gung Memorial Hospital, Keelung, Taiwan; ⁴School of Traditional Chinese Medicine, Chang Gung University, Kweishan, Taoyuan, Taiwan; ⁵Department of Chemical Engineering and Graduate Institute of Biochemical Engineering, Ming Chi University of Technology, New Taipei City, Taiwan; ⁶Department of Traditional Chinese Medicine, Xiamen Chang Gung Memorial Hospital, Xiamen, People's Republic of China; ⁷Chronic Diseases and Health Promotion Research Center, Chang Gung University of Science and Technology, Puzi, Chiayi, Taiwan; ⁸Department of Pathology and Laboratory Medicine, Taichung Veterans General Hospital, Taichung, Taiwan; ⁹School of Medicine, Chung Shan Medical University, Taichung, Taiwan; ¹⁰Department of Post-Baccalaureate Medicine, College of Medicine, National Chung Hsing University, Taichung, Taiwan; ¹¹Department of Dermatology, Yale School of Medicine, Yale University, New Haven, CT, USA; ¹²Pharmaceutics Laboratory, Graduate Institute of Natural Products, Chang Gung University, Kweishan, Taoyuan, Taiwan; ¹³Department of Anesthesiology, Chang Gung Memorial Hospital, Linkou, Taiwan

*These authors contributed equally to this work

Correspondence: Jia-You Fang, Pharmaceutics Laboratory, Graduate Institute of Natural Products, Chang Gung University, 259 Wen-Hwa 1st Road, Kweishan, Taoyuan, 333, Taiwan, Email fajy@mail.cgu.edu.tw

Purpose: Injectable deoxycholic acid (DA) has been approved for removing excess submental fat and is off-label for local adipose tissue reduction. Conventional DA injections fail to control fat reduction and generate severe adverse effects in adjacent non-adipose tissues. We designed squarticles as lipid-based nanoparticles for DA delivery to reduce fat accumulation.

Methods: The liquid lipid phase of the squarticles was composed of squalene, which was previously reported to sequester the toxicity of overdosed drugs. Rhein, a natural anti-adipogenic compound, was incorporated into the squarticles for combined fat-lowering.

Results: The squarticles had an average diameter of 93 nm and high rhein encapsulation (96%). The nanoparticles were easily internalized into mature adipocytes and were located in the lysosomes. DA induces adipocyte death via apoptosis and necrosis; however, nanoencapsulation can decrease cell death. Compared to free DA, squarticles showed superior mitigation of cytotoxicity against non-targeted cells (skin fibroblasts). Oil Red O staining indicated that squarticles loaded with DA or rhein alone inhibited lipid droplets by 42% and 17%, respectively. DA and rhein worked together in squarticles to further suppress fat accumulation by 50%. Dual administration of DA and rhein to the nanocarriers downregulated adipokines. The intraperitoneal administration of squarticles loaded with DA and rhein significantly decreased body weight, total cholesterol, and adipokine release. Histological analysis revealed that squarticles reduced adipocyte hypertrophy in the groin and epididymis by 11% and 53%, respectively. We examined the toxicity of the combination of DA+rhein in healthy rats that received a dose three-fold higher than that used in the pharmacological assessment. The survival rate of the overdosed DA+rhein increased from 50% to 100% after nanoencapsulation. Free compounds induce ascites, liver size reduction, AST/ALT elevation (1.5-fold), and potassium imbalance in rats. Nanoencapsulation significantly reduced these adverse effects.

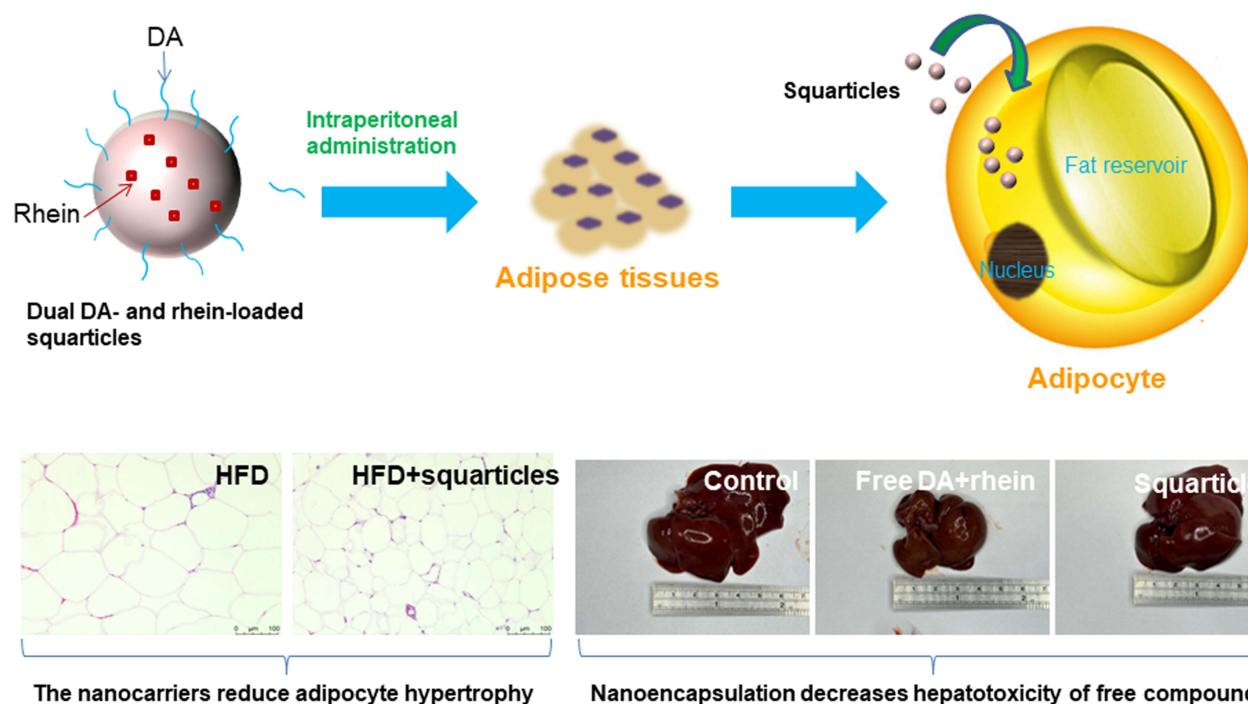
Conclusion: Our findings highlight the potential of squarticles for treating obesity.

Keywords: deoxycholic acid, rhein, squarticle, lipid-based nanoparticle, obesity, adverse effect

Introduction

Obesity is a metabolic disorder affecting 39% of the global population according to a report of the World Obesity Federation. It is a serious public health problem linked to an increased risk of diabetes, hypertension, cardiovascular

Graphical Abstract



diseases, dementia, depression, and tumors.¹ Approximately 20% of cancers are attributed to obesity.² Over the last few decades, anti-obesity drugs have been approved for obesity management. However, their use is usually accompanied by severe adverse effects such as nervousness, headache, and dizziness.³ These side effects have led to its withdrawal from the market. Moreover, excess fat accumulation in specific tissues persists even with the use of anti-obesity drugs. Submental fat accumulation can be described by the hypertrophy and hyperplasia of adipocytes, which are responsible for the dysfunction of lipid storage and inflammatory reactions.⁴ Suppressing adipocyte differentiation and decreasing adipocyte viability are strategies for inhibiting fat accumulation in tissues.⁵ Apoptosis and necrosis are vital factors in adipocyte depletion, which maintains homeostasis during fat reduction.⁶ Deoxycholic acid (DA) injection (Kybella) has been shown to reduce submental fat via adipocyte apoptosis or adipocytolysis.⁷ DA is an endogenous secondary bile acid. Synthetic DA was developed by the pharmaceutical industry for clinical applications. DA, an anionic surfactant, disrupts the adipocyte membrane to produce focal adipocytolysis, leading to loss of fat architecture.⁸ Although its approval is limited to submental fat reduction, DA has been applied off-label to treat lipomas, excess orbital fat, and abdominal adiposity.⁹

A major concern with DA use is that >97% of DA-treated patients experience adverse effects.¹⁰ The nonselective effect of adipose tissue-injected DA on adjacent tissues often induces severe side effects, including tissue fibrosis, vascular necrosis, skin necrosis, nervous lesions, and alopecia.¹¹ Nonspecific injury is the reason why DA injection is only approved for the treatment of small anatomic areas without extensive application. Therefore, there is an urgent need to design novel formulations for DA treatment in a safe and efficient way. Nanocarriers are a promising approach to achieve this goal. They have a large surface area, high bioavailability, good targeting of specific tissues, and controllable drug release, all of which are beneficial for the treatment of obesity.¹² The efficient delivery of drugs by nanomaterials has resulted in a reduction in the drug dose necessary to obtain the desired bioactivity, thus minimizing the side effects. Lipid- and silica-based nanoparticle encapsulation reduces surfactant toxicity of the surfactants.^{13,14} Another concern with the application of DA is the need for multiple injections and large volumes to

reduce fat. Moreover, maintaining adipocyte apoptosis at an appropriate level without redundant adipocytolysis is crucial for homeostasis. It is preferable for DA to be combined with another fat-reducing agent to exhibit synergistic activity with the aim of lowering the applied dose and causing excessive cell death. Phytochemicals are potential candidates for the treatment of obesity because they inhibit adipogenesis, lipolysis, and adipocyte apoptosis.¹⁵ Among these natural compounds, rhein, isolated from rhubarb, suppresses obesity by inhibiting adipocyte differentiation, reducing adipogenesis, and enhancing lipolysis.^{16,17} However, its clinical applicability is limited by poor water solubility and low bioavailability.¹⁸ To overcome these drawbacks, nanocarriers have been used for rhein delivery.¹⁹ The aim of this study was to develop nanocarriers loaded with DA and rhein for synergistic fat and toxicity reduction.

Nanostructured lipid carriers (NLC) have been employed as vehicles for DA and rhein because of their good tolerance in the body, controlled drug delivery, and possible large-scale production.²⁰ The incorporation of liquid and solid lipids in the matrix of NLC allows the efficient entrapment of large amounts of drug molecules and increases their stability.²¹ In this study, squalene and hexadecyl palmitate were used as the liquid and solid lipids, respectively, in the NLCs. Squalene is a polyunsaturated hydrocarbon with lipophilic properties and high biocompatibility. Natural oil in lipid nanoparticles (squarticles) has been reported to detoxify overdosed antidepressants.²² We expect that squalene in NLC may also be useful for reducing the side effects of DA. In this study, we developed squarticles loaded with DA and rhein, examined their toxicity, and evaluated their efficacy in reducing fat accumulation using both *in vitro* and *in vivo* assessment platforms.

Materials and Methods

Fabrication of the Squarticles

The preparation procedures of squarticles were modified from previous investigation.²³ The lipid phase of the squarticles contained squalene (2.7%, w/v of the final products), hexadecyl palmitate (0.9%), soybean phosphatidylcholine (1.8%), DA (0.098%), and rhein (0.0196%). The water phase consisted of the Poloxamer 188 (1.8%) and water. Both phases were heated to 85°C for 20 min. The water phase was added to the lipid phase and homogenized at 12,000 rpm for 30 min. The mixture was then sonicated using a probe-type sonicator at 35 W for 30 min. The final volume of each squarticle was 10 mL.

Physicochemical Property Determination of the Squarticles

By using the dynamic light scattering technique, the size, polydispersity index (PDI), and zeta potential of squarticles were detected at 25°C (Nano ZS90, Malvern). The squarticles were diluted 100-fold with water before measurement. For estimating the encapsulation efficiency of rhein, squarticles were centrifuged at 48,000 ×g at 4°C for 30 min to discard the free rhein in the supernatant. The precipitate with squarticle-entrapped rhein was dissolved in Triton X-100. The encapsulation percentage of rhein was quantified using high-performance liquid chromatography (HPLC). An HPLC system (Hitachi Series 2) equipped with a Merck LiChrospher C18 column was used for analysis. The mobile phase comprised a mixture of methanol and water containing 1% acetic acid (85:15). The flow rate and wavelength used for the rhein detection were 1 mL/min and 280 nm, respectively.

Cell Culture and Differentiation

3T3-L1 preadipocytes and Hs68 skin fibroblasts were purchased from the Bioresource Collection and Research Center, Taiwan. The cells were grown in Dulbecco's modified Eagle's medium (DMEM) supplemented with 10% fetal bovine serum (FBS), 1% antibiotics, and 1 mM sodium pyruvate. 3T3-L1 cells (1×10^4 cells/well) were cultured in 24-well plates for 2 days. Subsequently, the medium was changed to differentiation-induction medium composed of DMEM containing 10% FBS, 500 μM 3-isobutyl-1-methylxanthine, 0.25 μM dexamethasone, and 10 μg/mL bovine insulin (MDI). After a 2-day incubation, the medium was replaced by DMEM containing 10% FBS and 10 μg/mL bovine insulin. The 3T3-L1 cells were incubated for 4 days to induce differentiation.

Cell Viability Assay

The adipocyte viability was evaluated via the 3-(4,5-dimethylthiazol-2-yl)-2,5-diphenyltetrazolium bromide (MTT) analysis method. Cells were plated at 1×10^5 cells/well in a 96-well plate. The free or nanoparticulate DA (0–100 μM) and rhein (0–20 μM) were incorporated into the well and incubated for 24 h. Then the MTT reagent (5 $\mu\text{g}/\text{mL}$) was added into the well for 4 h. The culture medium was removed and formazan crystals were dissolved in dimethylsulfoxide (DMSO; 100 μL). The optical density was determined using a microplate reader at 570 nm.

Nanoparticle Uptake by Adipocytes

For tracing the squarticle uptake by the cells, rhodamine 800 (10 $\mu\text{g}/\text{mL}$) was used as the fluorescence dye to detect the nanoparticle internalization via flow cytometry and confocal laser scanning microscopy.²⁴ The nanoparticles were incubated with adipocytes (1×10^5 cells/well) for 24 h. The cells were centrifuged at $500 \times g$ for 10 min. The 3T3-L1 cell pellet was lysed using lysis buffer (0.5 mL/well). Fluorescence from a gated population of adipocytes (10,000 cells) was acquired using channel FL3 with excitation at 488 nm. Nanoparticle internalization was observed under a confocal microscope (TCS SP8 X AOBS, Leica). The 3T3-L1 cells were labeled with Hoechst 33342 (Thermo Fisher Scientific) and LysoTracker (Invitrogen) to visualize the nuclei and lysosomes, respectively.

Oil Red O (ORO) Staining

ORO staining was used to observe lipid droplet production in differentiated adipocytes.²⁵ 3T3-L1 cells were seeded in a 6-well plate at 8×10^4 cells/well. The free or nanoencapsulated DA (0–100 μM) and rhein (0–20 μM) were added into the well. After 48-h treatment, the adipocytes were washed with phosphate-buffered saline (PBS) and fixed with 10% formaldehyde. The fixed cells were stained with ORO working solution for 10 min and washed with water. The lipid droplets in the cells were dissolved in isopropanol and the absorbance was measured at 520 nm using a microplate reader.

Triglyceride (TG) Accumulation in Adipocytes

The methods of cell differentiation and treatment with DA and rhein were the same as those used for ORO staining. TG accumulation was determined using a TG colorimetric kit (Biovision), according to the manufacturer's protocol.

Enzyme-Linked Immunosorbent Assay (ELISA)

The protein expression of interleukin (IL)-1 β , IL-6, tumor necrosis factor alpha (TNF- α), and leptin in the supernatant of the adipocyte medium was detected by ELISA kits (BioLegend) according to manufacturer's instruction. The absorbance was determined at 450 nm using a microplate reader. The protein concentrations were estimated based on a standard calibration curve.

Immunoblotting Assay

Western blotting was performed using differentiated adipocytes after treatment with free or nanoparticulate DA (20 μM) and rhein (4 μM) for 24 h. The cells were washed twice with PBS and lysed in lysis buffer for 30 min. The cell lysate was centrifuged at 12,000 rpm for 20 min. The supernatants were collected for Western blot analysis. The amount of protein in the supernatant was quantified using the Bradford assay (Bio-Rad). The samples were electrophoresed on a 10% sodium dodecyl sulfate-polyacrylamide gel and the proteins were transferred onto a nitrocellulose membrane. The blots were blocked in PBS containing 5% skim milk and 0.5% Tween 20 for 1 h. The membrane was probed with a primary antibody (1:1000) for 24 h and horseradish peroxidase-conjugated secondary antibody (1:5000) for 1 h. The primary antibodies used in this experiment included peroxisome proliferator activated receptor (PPAR) γ and CCAAT/enhancer-binding protein (C/EBP) α , fatty acid synthase (FAS), acetyl-CoA carboxylase (ACC), caspase 3, caspase 9, and poly ADP-ribose polymerase (PARP). After washing with Tween 20-tris-buffered saline, protein bands were detected using an enhanced chemiluminescence kit (PerkinElmer). The protein concentration was calculated by the ratio of the densitometric measurement of the protein to that of the control protein (β -actin).

Apoptosis and Necrosis of Adipocytes

Apoptosis and necrosis were evaluated using flow cytometry.²⁶ Adipocytes treated with free or nano-encapsulated DA and rhein were harvested after incubation, washed with PBS, and suspended in a binding buffer. Annexin V and propidium iodide (PI) were added, and the cells were incubated for 20 min. The samples were analyzed via flow cytometry. Early apoptotic adipocytes were defined as annexin V-positive and PI-negative, whereas late apoptotic (necrotic) adipocytes were defined as annexin V-positive and PI-positive.

Animals

Five-week-old male Sprague Dawley rats were purchased from BioLasco (Taiwan). The animals were maintained in a humidity- and temperature-controlled room (55% at 25°C). The animal experiments were approved and conducted in strict accordance with the recommendations of the Guidelines for the Institutional Animal Care and Use Committee of Chang Gung University.

In vivo Intervention of Squarticles in Obese Rats

Twenty-six male rats were divided into four groups: (i) control (CTL): healthy rats were fed a standard diet for 8 weeks; (ii) high-fat diet (HFD): the rats were fed a HFD for 8 weeks, and PBS was intraperitoneally administered into the rats 2 times/week for the last 3 weeks; (iii) HFD+D+rhein: the rats were fed a HFD for 8 weeks, and free DA (20 mg/kg) and rhein (4 mg/kg) in DMSO/water (3:7) was intraperitoneally administered into the rats 2 times/week for the last 3 weeks; and (iv) HFD+squarticles+D+R: the rats were fed a HFD for 8 weeks, and squarticles containing DA (20 mg/kg) and rhein (4 mg/kg) in DMSO/water (3:7) was intraperitoneally administered into the rats 2 times/week for the last 3 weeks. The animals were weighed twice weekly. After an 8-week treatment, the animals were sacrificed to collect the plasma and organs for further assays. Organ weights were measured immediately after surgery.

Plasma Biochemical Analysis

Plasma was obtained from the rats by centrifugation (1500 ×g) at 4°C for 15 min. Total cholesterol in the plasma was estimated using a Dimension EXL2000 Integrated Chemistry analyzer (Siemens). The concentrations of aspartate aminotransferase (AST), alanine aminotransferase (ALT), blood urea nitrogen (BUN), and creatinine (CRE) were determined using laboratory kits (DRI-CHEM Slide, Fujifilm) on an automated analyzer (DRI-CHEM 4000i, Fujifilm).

Adipokines in Organs and Tissues

The levels of adipokines in the kidney, liver, spleen, groin, and epididymis were estimated using ELISA. After weighing, the minced organs and tissues were mixed with PBS as the extraction medium. The mixture was homogenized with ceramic beads using a MagNA Lyser (Roche).¹⁷ Supernatants of the homogenates were obtained by centrifugation (12,000 rpm) at 4°C for 10 min. The ELISA was performed according to the manufacturer's instructions. The adipokines detected in this experiment included IL-1 β , IL-6, TNF- α , and leptin.

Histology

Dissected liver and adipose tissues were fixed in a 10% neutral-buffered formaldehyde solution. The sections were stained with hematoxylin and eosin (H&E). Photomicrographs of H&E-stained sections were obtained using an optical microscope (DMi8; Leica). Images of H&E-stained sections were captured to analyze adipocyte size using the ImageJ software. The mean adipocyte size was expressed as the cross-sectional area per cell. The calculation was based on the values obtained from 20 adipocytes. Sections were prepared for immunohistochemical (IHC) analysis of FAS. Slices were incubated with an anti-FAS antibody (1:500) and treated with biotinylated donkey anti-rabbit immunoglobulin (Ig)G.

In vivo Toxicity Assay

The rats fed a normal diet were divided into three groups (six rats for each group): (i) CTL: the rats were intraperitoneally injected with PBS 2 times/week for 3 weeks; (ii) DA+rhein: the rats were intraperitoneally injected with free DA (60 mg/kg) and rhein (12 mg/kg) 2 times/week for 3 weeks; and (iii) squarticles+D+R: the rats were intraperitoneally injected with squarticles containing DA (60 mg/kg) and rhein (12 mg/kg) 2 times/week for 3 weeks. All animals were weighed twice per week for 3 weeks. The survival rate was also determined during the 3-week experiment. At the end of the experiment, the rats were sacrificed to collect plasma and organs/tissues to assess organ weight, total cholesterol, TG, biochemical markers, and histology.

Statistical Analysis

All data are reported as the mean and standard error of the mean. Differences in the data between the different treatment groups were analyzed using the Kruskal–Wallis test. Dunn’s test was employed as a post-hoc test to check for individual differences. Significance is indicated by $p < 0.05$ (*), 0.01 (**), and 0.001 (***)

Results

Physicochemical Properties of Squarticles

We prepared squarticles with or without fat-reducing agents, including DA and rhein. The squarticles without the bioactive compounds had an average particle size of 95 nm (Table 1). Incorporation of DA or rhein alone slightly reduced the particle size to 92 nm. The average diameter of the squarticles containing both active compounds was 93 nm. The PDI of all nanoformulations were below 0.3, demonstrating a homogeneous distribution of the nanoparticles. The PDI was higher after than before entrapment of the active agents. Owing to the presence of phosphatidylcholine, the surface of the squarticles exhibited a negative charge, according to the zeta potential. Incorporation of DA and rhein further increased the negative charge. The encapsulation percentage of rhein in the squarticles was 98%. Furthermore, the incorporation of DA into the nanoparticles did not significantly change this encapsulation percentage (96%).

Squarticles are Ingested by Adipocytes and Reduce the Cytotoxicity of DA

To evaluate the interaction and internalization of the squarticles by adipocytes, nanocarriers were loaded with fluorescent-labeled rhodamine 800 to emit red fluorescence. The cellular uptake of the nanoparticles was recorded via flow cytometry after incubation for 24 h. The histogram showed enhanced cellular uptake of DA-loaded squarticles compared to that of empty squarticles (Figure 1A). Squarticles+D was approximately two times greater in 3T3-L1 cells than in cells treated with empty nanoparticles (Figure 1B). We further monitored the uptake of nanoparticles via confocal microscopy. Adipocytes without nanoparticle incubation did not show rhodamine 800 fluorescence inside the cells (Figure 1C). Elevated red fluorescence was observed intracellularly after nanoparticle treatment. Both the squarticles and squarticles +D were successfully transferred into the cytoplasm. A large number of nanocarriers entered the adipocytes to co-localize with lysosomes (green signal), indicating that the lysosomes captured several nanoparticles.

The toxicity of free and nanoparticulate fat-reducing agents was evaluated using the MTT assay using adipocytes and skin fibroblasts. In the case of adipocytes, a dose-dependent decrease in cell viability was found when adipocytes were

Table 1 The Characterization of NLC by Nanoparticle Size, Polydispersity Index (PDI), Zeta Potential, and Rhein Encapsulation Percentage

Formulation	Size (nm)	PDI	Zeta Potential (mV)	Rhein Encapsulation (%)
Squarticles	94.8±0.9	0.22±0.04	-30.2±2.7	—
Squarticles+D	91.9±0.5	0.25±0.02	-50.6±0.7	—
Squarticles+R	91.9±0.6	0.26±0.01	-42.5±0.8	97.8±4.0
Squarticles +D+R	93.1±0.8	0.29±0.01	-40.3±1.3	95.5±5.9

Notes: Each value represents the mean±SEM (n=3).

Abbreviations: D, deoxycholic acid; R, rhein.

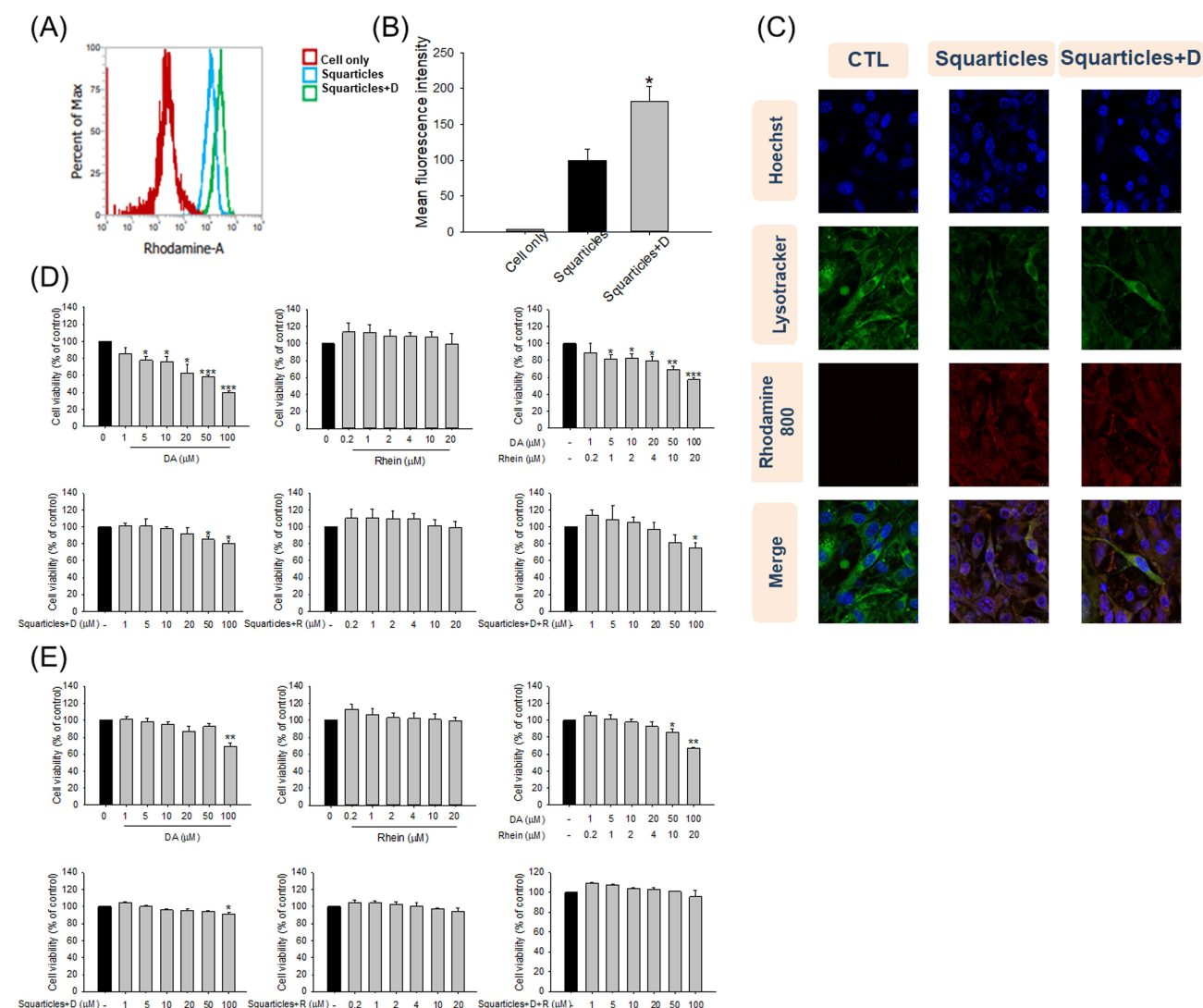


Figure 1 The cell uptake and cell viability after treatment of free DA and/or rhein solution or squarticles loaded with DA and/or rhein: **(A)** flow cytometry analysis of empty or DA-loaded squarticles incubated with 3T3-L1 cells; **(B)** the quantification of intracellular uptake of empty or DA-loaded squarticles in 3T3-L1 cells; **(C)** confocal microscopic images of empty or DA-loaded squarticles (red), DAPI (blue), and LysoTracker (green) showing uptake of nanoparticles by 3T3-L1 cells in 3T3-L1 cells; **(D)** the 3T3-L1 cell viability after treatment of free DA and/or rhein solution or squarticles loaded with DA and/or rhein as determined by MTT assay; and **(E)** the in skin fibroblast (Hs68) viability after treatment of free DA and/or rhein solution or squarticles loaded with DA and/or rhein as determined by MTT assay. All data are presented as the mean of three experiments \pm S.E.M. *** $p < 0.001$; ** $p < 0.01$; * $p < 0.05$ as compared to the control group.

treated with free DA (Figure 1D). Free DA at the highest dose (100 μ M) reduced adipocyte viability to 40%. 3T3-L1 cell viability was intact with the treatment of free rhein (0–20 μ M), suggesting a good tolerance. Similar to free DA alone, the combination of DA and rhein decreased the cell population growth in a dose-dependent manner. The adipocyte viability was not impaired by incubation with nanoencapsulated DA at 0–20 μ M. A significant reduction of viability was detected at 50 and 100 μ M. Nanoencapsulated rhein did not affect adipocyte viability, even at the highest concentration (20 μ M). Adipocyte viability was detected to remain >80% up to 50/10 μ M of squarticles loaded with dual DA and rhein (squarticles+D+R). Squarticles+D+R at the highest concentration (100 and 20 μ M) decreased adipocyte viability to 75%. This cytotoxicity was lower than that of the combined free forms. Hs68 fibroblasts were used as non-targeted cells to examine the cytotoxicity of DA and rhein. Free DA, alone or in combination with rhein, was cytotoxic to skin fibroblasts (Figure 1E). Similar to 3T3-L1 cells, the squarticles could shield the cytotoxicity of DA in Hs68 cells. These results indicated that squarticles loaded with DA were well tolerated by targeted and non-targeted cells.

Squarticles Inhibit Fat Accumulation and Adipokines in Adipocytes

To evaluate the impact of free and nanoparticulate DA and rhein on fat reduction, the intracellular accumulation of lipid droplets was observed using ORO staining. ORO analysis showed that the mature adipocytes had a distinct adipose phenotype (Figure 2A). Treatment with free DA inhibited lipid accumulation in 3T3-L1 cells in a dose-dependent manner, based on an evaluation of the microscopic images. Cell death was observed at higher doses of free DA. A minor decrease in fat was observed in the free rhein treatment group compared to that in the free DA group. The combination of free DA and rhein resulted in further fat reduction, manifesting a synergistic effect against lipogenesis. The number of intracellular lipid droplets decreased in the presence of quarticles+D (Figure 2B). However, quarticles+D inhibited fat accumulation to a lesser extent than the corresponding concentrations of free DA. Free and nanoencapsulated rhein caused similar inhibition of lipid droplets. The combination of DA and rhein in quarticles (quarticles+D+R) displayed less intense ORO staining than the nanocarriers loaded with DA or rhein alone. Quantification of lipid accumulation after ORO extraction further verified the microscopic observations (Figure 2C and D). Lipid deposition was decreased by 67% and 14% after treatment with free DA and rhein at the highest concentrations (100 and 20 μM), respectively. At the highest dose, the combination of free DA and rhein significantly reduced fat accumulation by 74%. The treatment with combined 100 μM DA and 20 μM rhein in quarticles resulted in a significant reduction in fat accumulation by 50% as compared to that of quarticles+D (42%) and quarticles+rhein (17%).

Intracellular TG was estimated after DA and rhein incubation for 24 h. Only the combinations of DA and rhein were examined in further experiments because they showed superior fat reduction efficiency than single agents. Both free and nanoparticulate forms of dual DA and rhein counteracted the synthesis in adipocytes (Figure 3A). This inhibitory action was evident starting from the DA dose of 1 μM . The TG produced in the adipocytes was significantly inhibited by 39% and 31% when free form and quarticles were added to the cells at the highest concentrations (100 μM DA and 20 μM rhein). We also estimated the changes in the protein levels of cytokines in adipocytes treated with free DA+rhein and quarticles. Adipocyte differentiation stimulated the expression of IL-1 β , IL-6, and TNF- α by 13-, 7-, and 14-fold over basal level (Figure 3B–D). The expression of cytokines was repressed after treatment with a combination of DA and rhein in a concentration-dependent manner, with the free form showing greater inhibition than nanoparticles. Leptin is another adipokine produced by mature adipocytes. We also observed a significant suppression of increased leptin levels in MDI-activated 3T3-L1 cells treated with a combination of DA and rhein (Figure 3E). To further investigate the effect of combined DA+rhein on adipocyte differentiation, we examined the protein level of the major adipogenic biomarkers PPAR γ , C/EBP α , FAS, and ACC in adipocytes. The differentiation significantly increased the protein expression of PPAR γ and C/EBP α (Figure 3F). This enhanced expression was remarkably attenuated by free DA+rhein but not by quarticles. Consistent with this tendency, the expression of FAS and ACC was inhibited by the free compounds but not by the nanocarriers (Figure 3G). This result demonstrates that quarticles containing DA and rhein could reduce fat accumulation; however, this effect was less than that of the free form, showing a limited influence on adipogenic marker attenuation.

Squarticles Induce Adipocytolysis Through Caspases/PARP Pathways

We aimed to explore the apoptotic/necrotic effects of a combination of DA and rhein on adipocytes and elucidate the underlying mechanisms. Early and late apoptosis (necrosis) of adipocytes treated with DA+rhein was analyzed via flow cytometry using Annexin V and PI. Compared to that in the non-treatment control, the proportion of apoptotic (Q4) and necrotic (Q2) cells was increased following the increase of free DA+rhein concentrations from 20 and 4 to 100 and 20 μM (Figure 4A). The cell death (apoptosis and necrosis) rate for the free forms with 20, 50, and 100 μM DA was 45%, 69%, and 84%, respectively (the right panel of Figure 4A). The nanoencapsulation significantly reduced the adipocyte death to 8%, 12%, and 42% for the 20, 50, and 100 μM DA, respectively. In the case of non-targeted skin fibroblasts, free compound-stimulated apoptosis and necrosis were higher than those in the quarticle-treated group (Figure 4B). The population of apoptotic/necrotic cells increased significantly in the free DA+rhein at 100 and 20 μM (the right panel of Figure 4B). This finding indicates that free DA+rhein is toxic to both targeted and non-targeted cells, raising concerns regarding the adverse effects on normal tissues or cells. Squarticles did not induce fibroblast death compared to that by

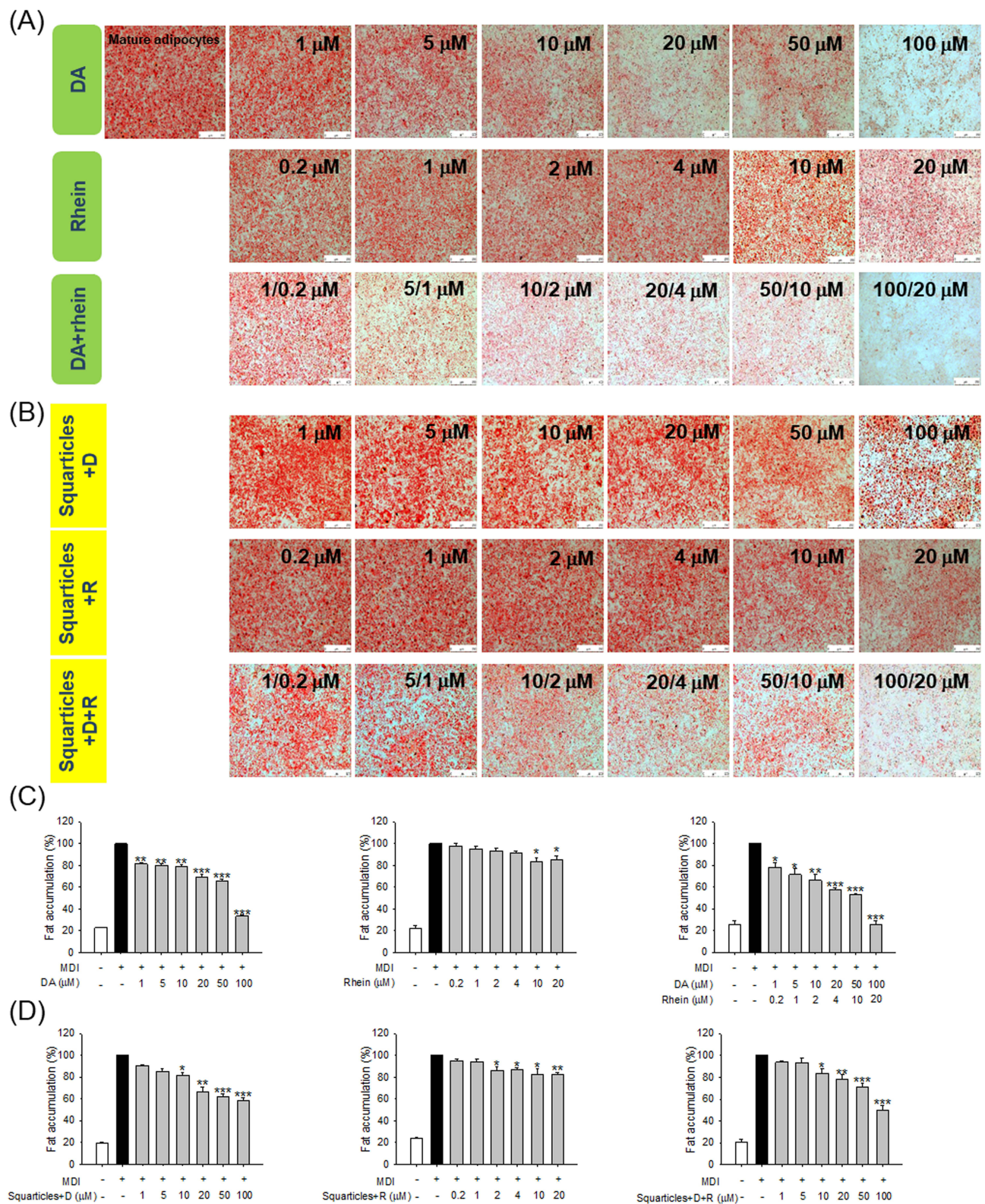


Figure 2 The fat accumulation in 3T3-L1 cells after treatment of free DA and/or rhein solution or squarticles loaded with DA and/or rhein as determined by ORO: (A) the ORO staining of 3T3-L1 cells after treatment of free DA and/or rhein solution with MDI stimulation; (B) the ORO staining of 3T3-L1 cells after treatment of squarticles loaded with DA and/or rhein with MDI stimulation; (C) the ORO quantification of 3T3-L1 cells after treatment of free DA and/or rhein solution with MDI stimulation; and (D) the ORO quantification of 3T3-L1 cells after treatment of squarticles loaded with DA and/or rhein with MDI stimulation. All data are presented as the mean of three experiments \pm S.E.M. *** $p < 0.001$; ** $p < 0.01$; * $p < 0.05$ as compared to the MDI-treatment group (mature adipocytes).

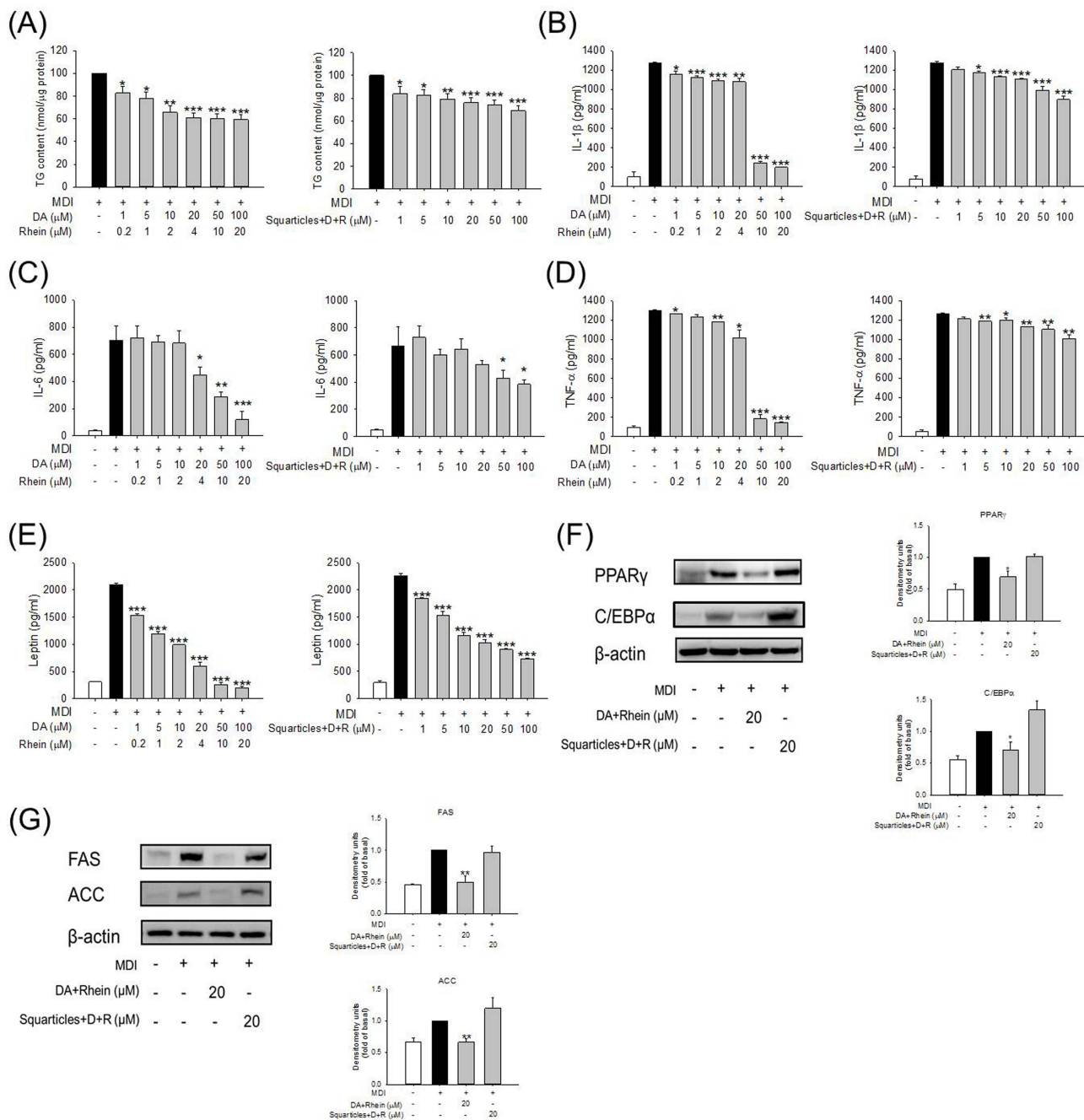


Figure 3 The effect of combined DA and rhein in free or nanoparticle form on adipokines and transcription factors of 3T3-L1 cells: **(A)** the intracellular TG content of 3T3-L1 cells after treatment of free or nanoparticle DA+rhein with MDI stimulation; **(B)** the IL-1 β expression of 3T3-L1 cells after treatment of free or nanoparticle DA+rhein with MDI stimulation; **(C)** the IL-6 expression of 3T3-L1 cells after treatment of free or nanoparticle DA+rhein with MDI stimulation; **(D)** the TNF- α expression of 3T3-L1 cells after treatment of free or nanoparticle DA+rhein with MDI stimulation; **(E)** the leptin expression of 3T3-L1 cells after treatment of free or nanoparticle DA+rhein with MDI stimulation; **(F)** the protein expression of PPAR γ and C/EBP α after treatment of free or nanoparticle DA+rhein with MDI stimulation; and **(G)** the protein expression of FAS and ACC after treatment of free or nanoparticle DA+rhein with MDI stimulation. All data are presented as the mean of three experiments \pm S.E.M. *** p < 0.001; ** p < 0.01; * p < 0.05 as compared to the MDI-treatment group (mature adipocytes).

the non-treated control. Furthermore, skin fibroblasts were more tolerant than adipocytes after treatment with DA and rhein.

Caspases are proteases that trigger apoptosis. Compared to the control, free DA+rhein treatment resulted in a significant increase in the expression of caspases 3 and 9 in a dose-dependent manner (Figure 4C). Squarticles did not change caspase 3 expression in adipocytes as compared to that in the control, whereas caspase 9 activity increased

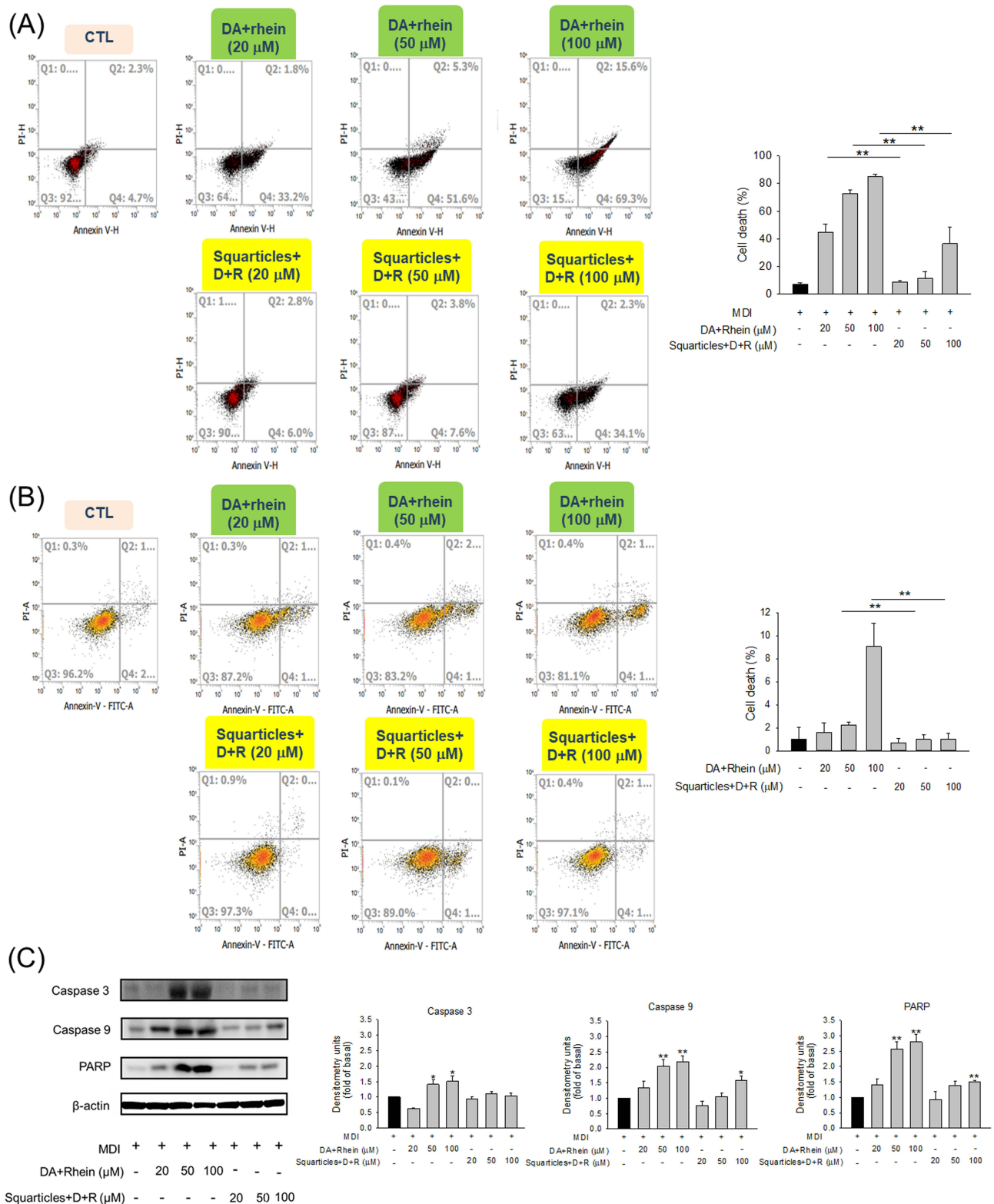


Figure 4 The effect of combined DA and rhein in free or nanoparticulate form on apoptosis and necrosis of 3T3-L1 cells and skin fibroblasts (Hs68): **(A)** 3T3-L1 cell death mechanism analysis using Annexin V and Propidium iodide through flow cytometry; **(B)** skin fibroblast death mechanism analysis using Annexin V and Propidium iodide through flow cytometry; and **(C)** Western blotting assay of caspase 3, caspase 9, and PARP in 3T3-L1 cells after treatment with combined DA and rhein in free or nanoparticulate form. All data are presented as the mean of three experiments \pm S.E.M. ****** $p < 0.01$ between the free and nanoparticulate forms (**A** and **B**). ****** $p < 0.01$ and ***** $p < 0.05$ as compared to the MDI-treatment group (mature adipocytes) (**C**).

slightly upon nanoparticle treatment at 100 μM DA. We calculated the relative protein expression levels of the apoptotic protein PARP. PARP cleavage increases cell disintegration. The level of cleaved PARP increased following treatment with free agents. The normal ratio of PARP increased by about 2.7-fold after the treatment of free forms at higher DA concentrations (50 and 100 μM). PARP also increased by 1.5-fold after the treatment of squarticles at 100 μM DA, while this upregulation was not detected in the case of lower doses (20 and 50 μM).

Combined DA and Rhein Mitigate Obesity and the Associated Inflammation in vivo

Next, we used an obese rat model to evaluate the in vivo efficacy of free and nanoparticulate DA+rhein for fat reduction via intraperitoneal injection. The body weight of the HFD-fed rats was significantly higher than that of the control rats (Figure 5A). This weight increase was significantly suppressed when free DA+rhein and squarticles were administered. The HFD-induced weight gain was reduced by 19% and 13% after treatment with the free form and squarticles, respectively, at the end of the experiment (57 days). We also measured the weight of the kidney, liver, spleen, and adipose tissues (groin and epididymis) at the end of the experiment. HFD increased the weights of the liver and adipose

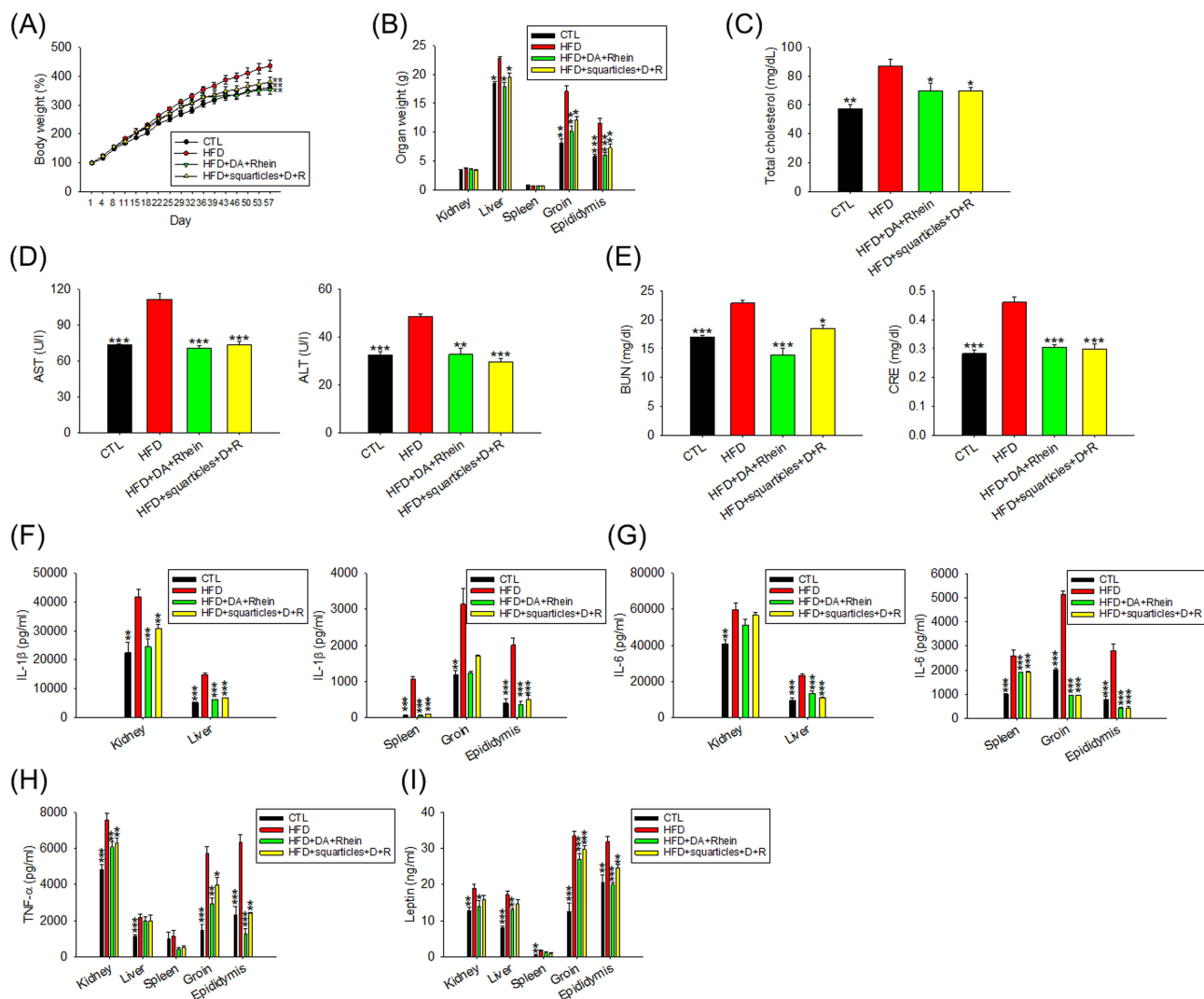


Figure 5 The antiobesity effect of combined DA and rhein in free or nanoparticulate form by intraperitoneal administration on the HFD-fed obese rats: **(A)** the body weight change as compared to normal diet group during the HFD-fed period; **(B)** the organ weight change as compared to normal diet group during the HFD-fed period; **(C)** total cholesterol in plasma after HFD consumption for 8 weeks; **(D)** AST and ALT concentration in plasma after HFD consumption for 8 weeks; **(E)** BUN and CRE concentration in plasma after HFD consumption for 8 weeks; **(F)** IL-1 β in organs/tissues after HFD consumption for 8 weeks; **(G)** IL-6 in organs/tissues after HFD consumption for 8 weeks; **(H)** TNF- α in organs/tissues after HFD consumption for 8 weeks; and **(I)** leptin in organs/tissues after HFD consumption for 8 weeks. All data are presented as the mean of six experiments \pm S.E.M. *** $p < 0.001$; ** $p < 0.01$; * $p < 0.05$ as compared to the HFD intervention alone.

tissues but not of the kidney and spleen (Figure 5B). The combination of DA and rhein significantly reduced the weight of the liver and adipose tissues in obese rats, with the free form showing a superior decline compared with squarticles. Biochemical serum analysis showed that both free and nanoparticulate DA+rhein remarkably reduced total cholesterol in HFD-fed rats to a comparable level (Figure 5C). Plasma levels of AST and ALT were higher in HFD-fed rats than in control rats. Free DA+rhein and squarticles reversed this increase to the baseline control levels (Figure 5D). The levels of biochemical markers in the kidney, BUN, and CRE, increased dramatically in the obese rats compared to the healthy group (Figure 5E). Treatment with the free form and squarticles reduced the BUN levels by 39% and 19%, respectively. The serum concentration of CRE in obese rats was remarkably decreased by free DA+rhein and squarticles to a similar level.

We also evaluated whether adipokine release in peripheral organs was influenced by dual treatment with DA and rhein. IL-1 β expression was significantly elevated in all organs examined after HFD intervention (Figure 5F). ELISA result showed that IL-1 β was significantly decreased in response to combined DA and rhein. Free form generally revealed a greater IL-1 β downregulation than the nanocarriers. The DA+rhein combination failed to inhibit IL-6 upregulation in the kidney after HFD feeding (Figure 5G), whereas it was effective in dampening IL-6 overexpression in other organs. In the case of IL-6, comparable inhibition by the free form and nanoparticles was observed. TNF- α expression was increased in the organs of HFD-induced obesity except spleen (Figure 5H). The combined DA+rhein could counteract TNF- α overexpression in kidney and adipose tissues but not in the liver. The free compounds exhibited a greater suppression of the overexpressed TNF- α than the squarticles in the adipose tissues. Similarly, leptin overexpression in the organs of obese rats was arrested by the combined treatment (Figure 5I). This inhibition was higher in the free than in the squarticle form; however, the difference was not statistically significant.

IHC Analysis Reveals a Fat-Reducing Effect of Combined DA and Rhein

We further examined the histology of the liver and adipose tissues following the administration of free and nanoencapsulated DA+rhein. Livers from the normal diet group displayed an arrangement of hepatocytes with an intact appearance (Figure 6A). The liver of HFD-fed rats showed a paler tone than that of healthy rats. This finding indicated hepatocellular damage and steatosis. HFD resulted in increased lipid accumulation in the hepatic tissue. Combined DA+rhein in free or nanoparticulate forms can repress steatosis. No histological differences were observed between healthy controls and squarticle-treated livers. IHC for FAS in hepatic tissue was also performed. HFD increased FAS distribution in the liver (Figure 6B). Treatment with free and nanoencapsulated DA+rhein reduced FAS overexpression, implying that the inhibition of lipogenesis by these compounds abrogated the fatty liver. The effect of the combined compounds on adipocyte hypertrophy was visualized using the H&E-stained slices of the adipose tissues. HFD significantly increased adipocyte size in the groin and epididymis (Figure 6C and D). The shrinkage of hypertrophied adipocytes was observed after treatment with a combination of DA and rhein. The average size of adipocytes in groin (221 μm^2) of obese rats was reduced to 207 and 196 μm^2 by injection of free form and squarticles, respectively (the right panel of Figure 6C). Supplementation with free form and the nanocarriers resulted in a notable reduction in the adipocyte size of epididymis from 299 to 193 and 142 μm^2 , respectively (the right panel of Figure 6D).

Nanoencapsulation Reduces the Toxicity of DA and Rhein

Finally, we examined the possible toxicity of the intraperitoneal administration of DA+rhein in healthy rats. The dose of DA+rhein used for the toxicity assay was three-fold higher than that used for the in vivo pharmacological analysis. The survival rate of animals receiving the free compounds gradually decreased over 22 days according to Kaplan-Meier curve (Figure 7A). The y-axis of this curve illustrated the probability of survival ranging from 0% to 100% for comparison of different treatment groups. The survival rate of rats treated with the free compound was 50% after 22 days. No animal deaths were observed after administration of squarticles containing DA+rhein, indicating a reduction in toxicity by nanoencapsulation. Body weight decreased by 28% when the free form was administered to the rats (Figure 7B), whereas no significant weight loss was observed in the nanoparticle group. The gross appearance of the rats revealed the presence of ascites in the abdominal cavity after the free-form treatment (Figure 7C). The animals were sacrificed after 22 days to excise their organs. Both kidneys in all groups were congested with a smooth capsule (Figure 7D). Kidney size was

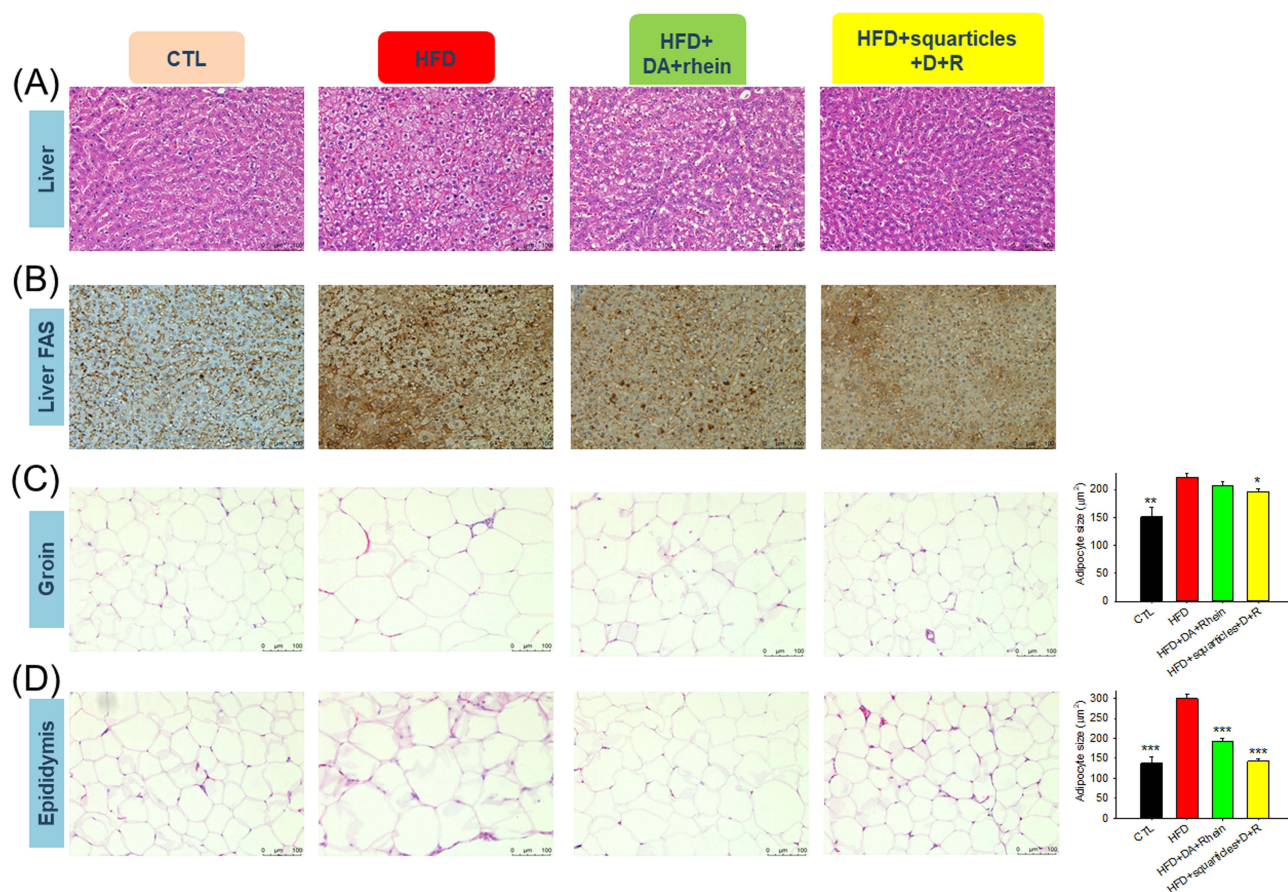


Figure 6 Histological examination of the HFD-fed obese rats after the intraperitoneal administration of combined DA and rhein in free or nanoparticulate form: **(A)** H&E staining of liver; **(B)** FAS expression of the liver determined by IHC; **(C)** H&E staining of groin; and **(D)** H&E staining of epididymis. All data are presented as the mean of six experiments \pm S.E.M. *** $p < 0.001$; ** $p < 0.01$; * $p < 0.05$ as compared to the HFD intervention alone.

similar among the three groups. The livers of the untreated control rats were congested and showed normal architecture. Liver size was reduced after exposure to DA+rhein, with the free form exhibiting a more significant reduction than the squarticles (Figure 7E). A similar trend was observed in the spleen (Figure 7F). The kidney and liver weights were significantly lowered by intervention with free DA+rhein (Figure 7G).

Biochemical and hematological parameters of the rats were analyzed. The free form significantly decreased the total cholesterol and TG levels in the plasma (Figure 8A and B). Serum cholesterol levels remained within the normal range in rats treated with the nanocarriers. A slight but significant reduction in TG was observed in the nanoparticle group compared with that in the control group. AST and ALT levels were significantly increased by approximately 1.5-fold after free form treatment for 22 days (Figure 8C). No significant changes were found in the AST and ALT levels between the squarticle-treated and control groups. In contrast to the pharmacological evaluation in obese rats, free DA+rhein increased BUN and CRE levels in a toxicological study at a three-fold dose (Figure 8D). The total protein and albumin levels in the serum decreased after free-form treatment (Figure 8E and F). The injection of squarticles did not change the total protein and albumin levels compared with the non-treatment control. High doses of the free compounds increased serum potassium, but not sodium (Figure 8G and H). In contrast, the lipid nanocarriers caused no changes in serum electrolytes.

Histological examinations of the organs retrieved from the rats were also performed. Representative microscopic findings of the kidney showed no observable lesions or morphological changes after treatment with a combination of DA and rhein (Figure 9A). No definite lobular inflammatory cell infiltration or cholestasis was observed in the livers of any of the treatment groups (Figure 9B). Liver plate atrophy or collapse was noted in the free-form-treated animals. There was no significant difference in the hepatic morphology between the control and squarticle-treated groups. To further

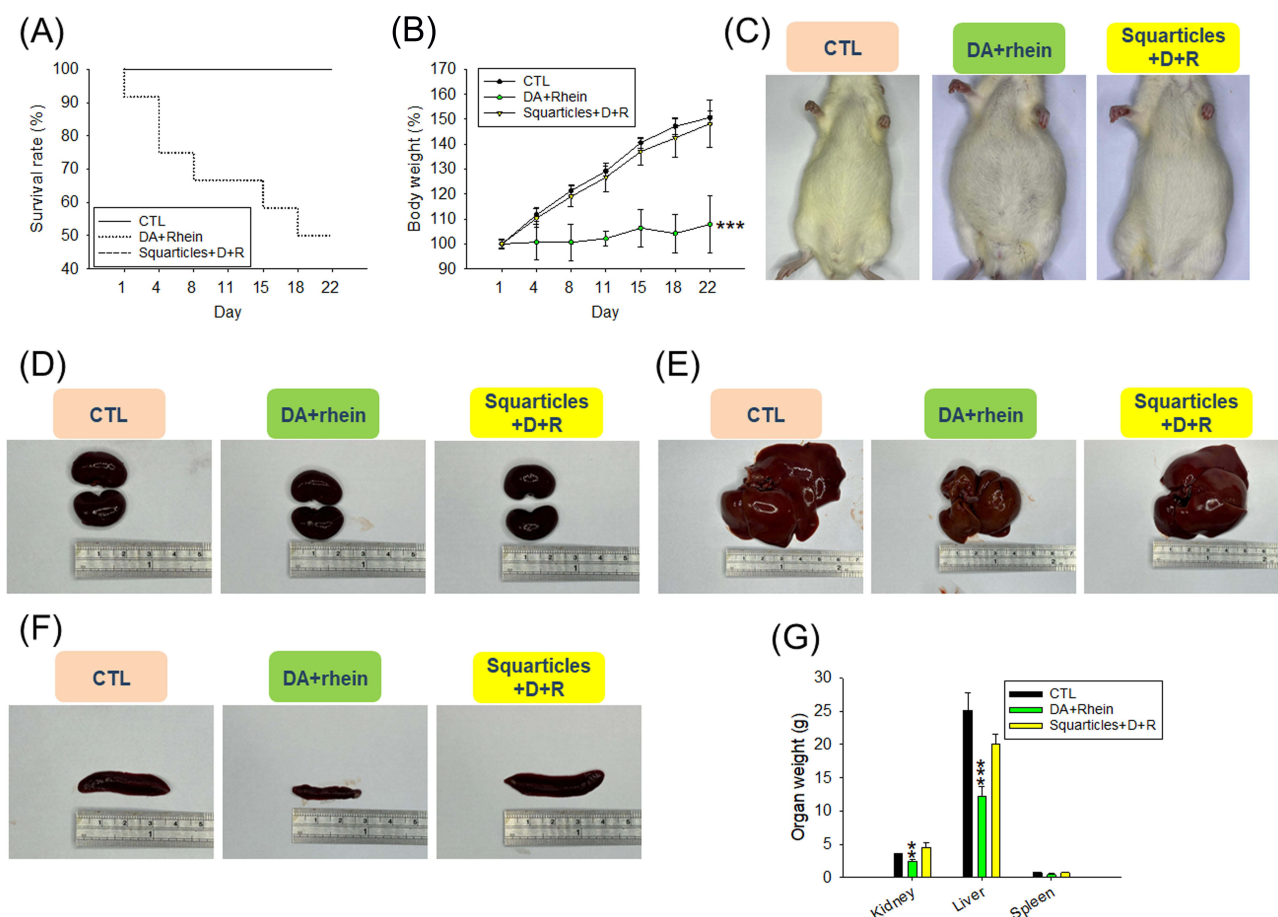


Figure 7 The safety assessment of combined DA and rhein in free or nanoparticulate form by intraperitoneal administration on the healthy rats: **(A)** the survival rate during 22 days; **(B)** the body weight change during 22 days of repeated (6 times) administration; **(C)** the gross appearance of the rats after 22 days of repeated (6 times) administration; **(D)** the gross appearance of the kidney after 22 days of repeated (6 times) administration; **(E)** the gross appearance of the liver after 22 days of repeated (6 times) administration; **(F)** the gross appearance of the spleen after 22 days of repeated (6 times) administration; and **(G)** the organ weight after 22 days of repeated (6 times) administration. All data are presented as the mean of six experiments \pm S.E.M. *** $p < 0.001$ and ** $p < 0.01$ as compared to the non-treatment control.

explore possible plate collapse, we stained the liver slices with reticulin IHC. Reticulin fibers can be used as indicators of liver architecture. We observed smaller liver cells and a narrower hepatic plate in IHC sections treated with the free form than in healthy controls (Figure 9C). The squarticle-treated liver showed a similar liver cell size and hepatic plate to that of the untreated control. Microscopic observation of the spleen sections showed that the intervention of free and nanoencapsulated DA+rhein did not alter the morphology and structure compared to the control (Figure 9D).

Discussion

The drastic increase in the prevalence of obesity has prompted investigations to focus more on pharmacotherapy to reduce fat accumulation. However, the use of current fat-reducing drugs is limited by their nonspecificity and unsustainable weight loss. DA effectively induces fat reduction through adipocytolysis. Nevertheless, this agent also damages normal tissues around obese tissues, causing adverse effects. DA disrupts adipose tissue homeostasis. DA injection is only approved for application in small areas, such as the submental fat; the use of DA in large areas is limited because of its unwanted toxicity. To date, very few investigations have been conducted on the design of DA formulations for appropriate pharmaceutical development. Nanocarrier systems could be an alternative approach to overcome the drawbacks of conventional anti-obesity drugs in reducing fat. Lipid-based nanoparticles are among the most clinically advanced delivery systems for drugs and nucleic acids, and their efficacy strongly depends on the lipid components. As compared to the other lipid-based nanosystems such as liposomes, NLC with lipid core can load more lipophilic agents such as ad rhein with high encapsulation efficiency. The lipid nanovesicles with aqueous core usually have limited

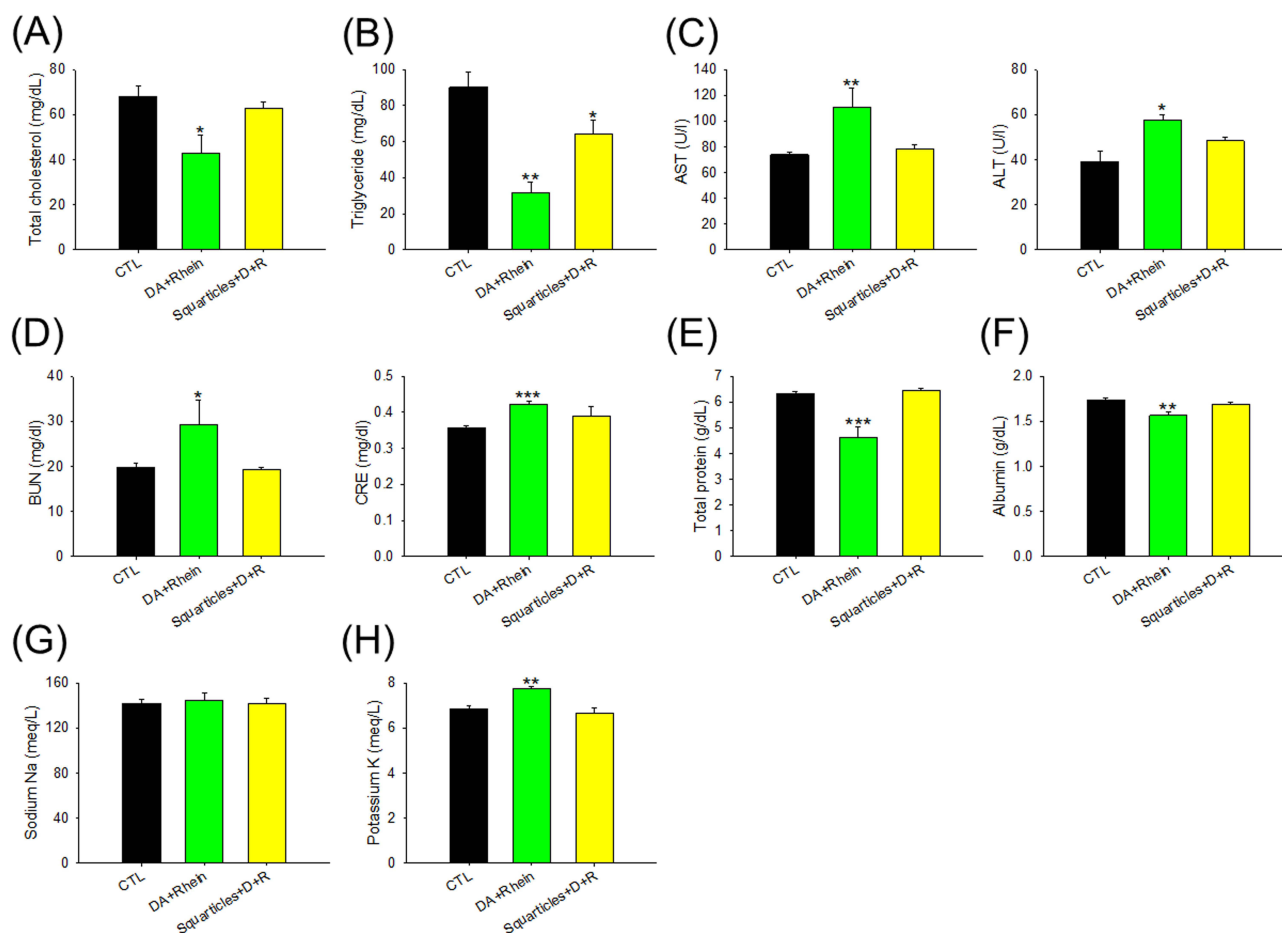


Figure 8 The biochemical serum analysis of combined DA and rhein in free or nanoparticulate form by intraperitoneal administration on the healthy rats: **(A)** total cholesterol in plasma after 22 days of repeated (6 times) administration; **(B)** TG in plasma after 22 days of repeated (6 times) administration; **(C)** AST and ALT concentration in plasma after 22 days of repeated (6 times) administration; **(D)** BUN and CRE concentration in plasma after 22 days of repeated (6 times) administration; **(E)** total protein concentration in plasma after 22 days of repeated (6 times) administration; **(F)** albumin concentration in plasma after 22 days of repeated (6 times) administration; **(G)** sodium concentration in plasma after 22 days of repeated (6 times) administration; and **(H)** potassium concentration in plasma after 22 days of repeated (6 times) administration. All data are presented as the mean of six experiments \pm S.E.M. *** $p < 0.001$; ** $p < 0.01$; * $p < 0.05$ as compared to the non-treatment control.

space for lipophilic agent entrapment. This study investigated the use of DA-loaded lipid nanocarriers composed of squalene for inhibiting lipogenesis inhibition. Squalene in the nanoparticles has been reported to reduce drug-induced toxicity.²² Rhein, an adipogenesis inhibitor, was incorporated into squarticles to reduce fat accumulation synergistically. Our results demonstrated that although the fat-reducing effects of DA and rhein were partly compromised by this nanoencapsulation, the squarticles had high tolerability and reduced side effects on adipocytes. In an in vivo obese animal model, squarticles showed antiadipogenic effects comparable to those of free DA and rhein. Nanoencapsulation of an overdose of DA and rhein remarkably diminished the death rate in mice. Based on the in vitro and in vivo results, squarticles were found to be effective and safe for the treatment of obesity.

The encapsulation efficiency of lipid-based nanocarriers is significantly affected by the drugs and their interactions with lipids.²⁷ An encapsulation percentage $>60\%$ often indicates the success of NLC preparation for loading an appropriate amount of drug molecules.²⁰ Our squarticles showed high rhein encapsulation ($>95\%$), suggesting that rhein has a high affinity for the lipid phase of squarticles. Lipophilic rhein molecules are homogeneously solubilized in the lipid matrix. The ratio of liquid lipid (squalene) to solid lipid (hexadecyl palmitate) in the squarticles was 3:1. The incorporation of liquid lipids into solid lipids results in massive disturbances in the crystalline order and lattice imperfections. A greater distance between the fatty acid chains and the spaces produced by imperfections in the lipid matrix is critical for loading abundant drug molecules.²⁸ The squarticles revealed a particle size <100 nm. An increase in liquid lipids in NLC is believed to lead to a decrease in the particle size.²⁷ This behavior can be attributed to the fact that

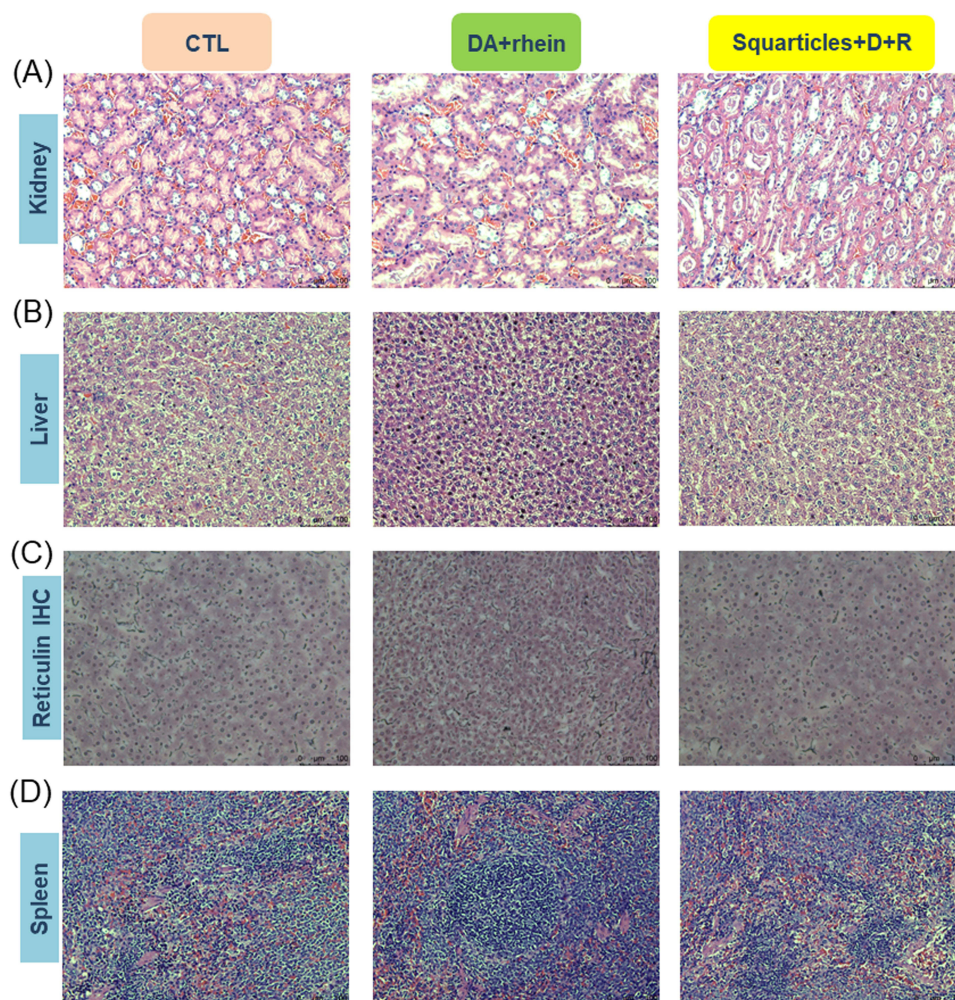


Figure 9 Histological examination of healthy rats after the intraperitoneal administration of combined DA and rhein in free or nanoparticulate form: (A) H&E staining of kidney; (B) H&E staining of liver; (C) reticulin expression of the liver determined by IHC; and (D) H&E staining of spleen.

more solid lipids affect the melting process and create aggregates during the NLC fabrication. Poloxamer 188, a non-ionic surfactant incorporated into squarticles, could also reduce the size owing to tight molecular packing with lipids. The addition of poloxamer 188 to NLC also resulted in low toxicity and sufficient biocompatibility.²⁹ The incorporation of DA and rhein slightly reduced particle diameter. Thus, we inferred that DA and rhein may possess co-surfactant characteristics that are negatively correlated with size. Nanoparticles with diameters between 50 and 200 nm are beneficial for drug delivery to biological systems because NLC <10 nm are cleared by the kidney and NLC >200 nm are recognized by the mononuclear phagocyte system.²⁸ The squarticles fit the feasible range for biological use. The stable NLC for prolonged storage should have a minimum zeta potential of ± 20 mV to maintain the electrostatic repulsion between particles.²⁹ Our nanoparticles fit this criterion. Poloxamer 188 also plays a role in repelling nanoparticle attraction through bulky steric repulsion.

To investigate the effect of squarticles on fat reduction in a cell-based study, differentiated 3T3-L1 cells were used, because this cell line is a standardized model for studying adipogenesis.³⁰ Lipid reduction in adipocytes can involve two mechanisms: adipogenesis inhibition and adipocyte destruction.⁹ Adipogenesis in adipocytes is determined by TG accumulation. TG is the major form of fatty acid stored in the lipid droplets of differentiated adipocytes. Redundant TG deposition in adipocytes prompts obesity development.³¹ ORO staining and TG detection demonstrated that free DA and rhein had the ability to decrease lipogenesis in adipocytes. Rhein ameliorates obesity via adipogenesis suppression.¹⁷ Rhein is a lipophilic compound that easily permeates adipocytes to inhibit adipogenesis. Free DA solutions, such as

commercial preparations (Kybella), are a micellar form that can be used for injection. Naked DA molecules can directly interact with the adipocyte membrane for adipocytolysis, with the destroyed adipocytes no longer storing fat. Cellular uptake experiments showed that the squarticles were largely internalized into differentiated 3T3-L1 cells. The size of the squarticles (approximately 90 nm) was suitable for increased cellular uptake, as a previous study²⁰ suggested that NLC should have a diameter range of 50–300 nm for cellular intake. Previous studies^{32,33} demonstrated a facile ingestion of squalene into cells in both free and nanoparticle forms. Squalene is a precursor of cholesterol. Cholesterol is accounted for about 40% of the cell membrane for structure maintenance and elasticity. Squalene might show strong interaction with the cell membrane for proficient uptake. After the endocytosis of lipid nanoparticles by cells, the nanoparticles enter the lysosomes, and lipid ionization at low pH enables lysosomal escape. This process allows the cargo to be released into the cytoplasm.³⁴ Confocal microscopy revealed the presence of squarticles in the lysosomes. The cationic surface charge of nanoparticles is usually preferred for cellular internalization because of electrostatic interactions with the cell membrane. Our data verified that the negative charge of the squarticles also impelled adipocyte uptake. The affinity between the lipids of squarticles and phospholipids in the cell membrane may be strong enough to facilitate cellular uptake. Entrapment by squarticles reduced the ability of DA and rhein to decrease the number of lipid droplets in adipocytes. Nanoparticle encapsulation reduced the direct contact between DA/rhein and the cell membrane, thereby decreasing adipocytolysis. Nevertheless, the combined effect of DA and rhein on lipogenesis inhibition was still observed after nanoparticle inclusion. Fewer injection frequencies and lower injection volumes can be achieved by incorporating rhein into DA formulations to reduce its adverse effects.

PPAR γ and C/EBP α play important roles in the early stage of adipocyte differentiation. Both these biomarkers provide positive feedback to orchestrate adipogenic schemes.³⁵ The combination of free DA and rhein significantly downregulated the expression of PPAR γ and C/EBP α induced by MDI; however, squarticles appeared to have less effect on this expression. DA and rhein are already proven to act as PPAR γ antagonists.^{16,36} This effect might be partly shielded by nanoparticle loading, resulting in the insignificant PPAR γ and C/EBP α downregulation. A similar tendency was observed for the downregulation of FAS and ACC expression. Both proteins are PPAR γ -targeted lipogenic factors that are associated with TG storage, fatty acid biosynthesis, energy expenditure, and glucose metabolism.³⁷ PPAR γ is essential to modulate the expression of cytokines for promoting adipocyte differentiation.³⁸ Adipocytes are fundamental to produce proinflammatory cytokines such as IL-1 β , IL-6, and TNF- α . These adipokines are upregulated in the adipose tissues of individuals with obesity and cause obesity-associated dysfunction.³⁹ Our data showed that squarticles significantly downregulated these cytokines in a dose-dependent manner; however, this effect was lower than that of the free form. DA-induced adipocyte damage by DA itself can abrogate cytokine production in adipocytes.³⁶ Rhein is reported to attenuate IL-1 β , IL-6, and TNF- α in the activated macrophages.⁴⁰ This effect was detectable in differentiated 3T3-L1 cells. Leptin is an adipose tissue hormone that is categorized as an adipokine. It stimulates pro-inflammatory cytokine production in adipocytes.⁴¹ The quantity of leptin secreted by adipose tissue is positively correlated with adipocyte size and lipid content. The injection of DA was confirmed to reduce leptin levels in adipose tissues.⁴² The inhibition of lipid and adipokine secretion by nanocarriers is an effective therapeutic approach for obesity.

In addition to biochemical mechanisms, anti-adipogenic action occurs through adipocyte death. Adipogenesis is involved in adipocyte differentiation and proliferation. The cytotoxicity of adipocytes in obesity is imperative to maintain homeostasis by eliminating unnecessary cells.⁴³ Significant adipocyte death was observed after treatment with free or nanoencapsulated DA. This detergent is cytotoxic via irreversible disruption of cellular and mitochondrial membranes.^{9,44} Thus, necrosis may be the predominant cause of adipocyte death following DA treatment. Cell death, including necrosis and apoptosis, involves the cleavage of proteins and DNAs. Necrosis is considered uncontrolled and is associated with cell membrane lysis. In contrast, apoptosis was associated with the expression of characteristic marker genes. A subgroup of effector caspases cleaves target proteins to elicit apoptosis.⁴⁵ Caspase 3 is an apoptotic signal transducer in 3T3-L1 cells. Apoptosis induces effector caspase 3 by cleaving procaspase 9 and generating active caspase 9 via an endogenous pathway.⁴⁶ PARP is a marker of cell disintegration and apoptosis and is targeted by caspase 3. Immunoblotting demonstrated the upregulation of caspase 3, caspase 9, and PARP following DA treatment in adipocytes, indicating the involvement of the apoptotic pathway. However, an earlier investigation⁵ indicated that DA did not activate apoptosis in 3T3-L1 cells. This effect could be due to the high DA concentration (2.55 mM) used in the previous

study. High DA concentration directly induces cell membrane lysis leading to necrosis. In the present study, low DA concentrations (20–100 μM) were used to treat adipocytes. Total membrane lysis was not observed at these DA concentrations; however, the apoptotic pathway occurred during this stimulation.

Rhein has been reported to induce apoptosis in both hepatocytes and cancer cells.^{19,47} In vitro cell viability test indicated that the adipocytes could tolerate up to 20 μM of rhein, suggesting a low cell death rate. Adipocyte apoptosis induced by squarticles treated with DA+rhein could be derived from the effect of DA but not of rhein. We also found that squarticles were less toxic than free DA and rhein, causing skin fibroblast death. One of the most severe adverse events associated with DA injections is skin ulceration.⁸ Nanoencapsulation of DA is expected to reduce skin necrosis. DA molecules were immobilized by the nanoparticles on the particulate surface. A significant interaction of DA in squarticles reduced the direct exposure of naked DA molecules on the cell membrane, thereby decreasing cell lysis. We also found that 3T3-L1 cells were more vulnerable to DA than fibroblasts. Adipocytes are more sensitive than keratinocytes, skin fibroblasts, and muscle cells because fat lacks specific proteins that bind to DA and neutralize its toxicity.⁴⁸

HFD rats treated with a combination of DA and rhein showed a decrease in body weight, total cholesterol, AST, ALT, BUN, CRE, and adipokines. Simultaneously, fat mass accumulation in the liver and adipose tissues of obese animals was arrested by this combination. These findings suggest that DA+rhein in the free or nanocarrier form effectively supports the prevention or management of obesity. After administration into the peritoneal cavity, the nanoparticles distributed to the tissues/organs in the cavity and then were ingested by the cells to induce signaling pathway for mitigating lipogenesis. The negative charge of the nanocarriers reduces the adsorption of opsonins onto the surface,⁴⁹ reducing the clearance from the body. The inflammatory cascade is activated in obesity.⁵⁰ Body fat deposition increases with a consequent elevation in adipokine secretion proportional to the increased size of adipocytes. The high levels of IL-6, TNF- α , and leptin are linked with the expansion of adipose tissues.⁵¹ Adipose tissues are important metabolic and immune organs that are critical for energy homeostasis as they act as reservoirs for lipids and adipokines.³⁹ Inflammation in adipose tissues due to excess secretion of IL-6 and TNF- α is a main factor to develop diabetes, insulin resistance, cancer, and obesity.³⁵ Leptin is primarily generated by adipose tissue, and its concentration is correlated with fat mass in the body.⁵² We examined the adipokines in both subcutaneous (groin) and visceral (epididymis) adipose tissues. The results revealed a significant decrease in adipokines in the adipose tissues of HFD-fed rats after the administration of free and nanoencapsulated DA+rhein. Under in vivo obesity conditions, the cytokine levels in adipose tissues are a summary of adipocytes and immune cells. Abundant fat storage promotes an increase in the number of neutrophils and macrophages in adipose tissue. Recruitment of macrophages in adipose tissues is associated with the increased IL-6 and TNF- α .⁵³ The combination of DA and rhein may be beneficial for suppressing cytokines released from both adipocytes and immune cells.

In addition to adipose tissue, obesity is associated with elevated inflammation in the hepatic tissue. Liver is a vital organ that regulates lipid homeostasis. Accumulation of lipids secreted from adipose tissues in the liver.⁵⁴ Our data also showed significant attenuation of cytokines in obese animals treated with the combined compounds. Rhein has been reported to alleviate the inflammatory response of macrophages activated by lipopolysaccharides.⁵⁵ An animal study of sepsis also indicated that rhein reduced IL-1 β , IL-6, and TNF- α in plasma and colon induced by lipopolysaccharides.⁵⁶ A reduction in pro-inflammatory cytokines in the liver is especially favorable for counteracting chronic inflammation associated with obesity and metabolic syndrome. The attenuation of obesity in HFD-fed rats led to a significant reduction in AST and ALT, which are hepatic inflammation biomarkers. The levels of BUN and CRE, which are biochemical markers of renal function, in obese rats were also decreased by the combination of DA and rhein. Rhein prevents chronic kidney disease in rats by inhibiting BUN and CRE via antioxidant mechanisms.⁵⁷

The primary lipogenic tissues in the body are the liver and adipose tissues. Lipogenesis is an integral part of the lipid interplay between the liver and adipose tissue, which maintains endocrine homeostasis.⁵⁸ We examined the histology of the liver and adipose tissues of HFD-fed rats. Rhein exhibits hepatoprotective activity against hepatic fibrosis and fatty liver.¹⁸ FAS expression is enhanced in the livers of patients with fatty livers.⁵⁹ The histology of the liver sections showed decreased steatosis and FAS expression after treatment with DA+rhein. An increase in the adipocyte size (hypertrophy) is a typical symptom of adipogenesis. Histological observation of the groin and epididymis showed a decrease in adipocyte size following the combined DA+rhein treatment. This effect has also been reported in patients receiving commercial DA

injections.⁹ The size reduction by the squarticles was greater than that of the free compounds. Clinically, DA injection causes extensive eradication of adipocytes with severe fibrotic scarring in subcutaneous adipose tissues.⁶⁰ The non-adipocyte reaction to DA suggests non-selectivity. However, this phenomenon was not observed in the present study. A low DA dose and nanocarrier entrapment could minimize excessive adipocyte eradication while maintaining the fat-reducing efficiency of DA.

Although DA is an adipocytolytic agent that reduces the volume of subcutaneous adipose tissue, its nonspecific features are always associated with damage to non-adipose tissues. Thus, improving the applicability of injectable DA is necessary because it is in direct contact with the cells in the organism. We evaluated the toxicity of combined DA and rhein in rats by exposing the rats to a three-fold higher concentration than that used for the pharmacological analysis. We found that the free compounds reduced the survival rate and total cholesterol, TG, total protein, and albumin levels. Squarticles containing DA and rhein generally showed no change in these toxicological indicators. The kidneys and liver are the most critical organs for the excretion or metabolism of toxic substances. Free compounds, but not nanoparticles, stimulated the biochemical factors in the kidneys and liver (BUN, CRE, AST, and ALT). Free DA+rhein showed the opposite results for these biochemical factors in the toxicological and pharmacological evaluations. These opposite effects can be attributed to the different doses used in these investigations. Lower doses have a therapeutic effect, whereas overdoses result in toxicity. Rhein exhibits bidirectional regulation in the kidneys and liver.¹⁸ This regulation depends on the dosage and treatment duration of rhein. Rhein possesses antioxidant properties and is bioactive. However, a high dose of rhein induces oxidative stress, impairing mitochondrial and hepatic functions.⁶¹ The kidneys play a vital role in maintaining fluid and electrolyte balance in the body. Serum potassium levels increased following exposure to free DA+rhein. Increased serum potassium levels has indicated nephrotoxicity and tissue damage.⁶² However, we observed no renal damage according to organ appearance and histology. The kidney disruption caused by free DA and rhein can be categorized as mild; nevertheless, nanoencapsulation by squarticles can retard this adverse effect.

Liver size and weight significantly decreased after treatment with the free compounds. Histological assays revealed disorder in the liver plate and collapse in the free compound-treated group. The reticulin structure that maintained the liver plate was destroyed, resulting in dysfunction in supporting the liver plate, which was the reason for the reduction in liver size. The spleen plays an essential role in the maintenance of homeostasis by recycling blood cells and fighting pathogens. Similar to its effect to the liver, free DA+rhein decreased spleen size; however, this effect was not observed in squarticles. We validated that the squarticle delivery of DA and rhein could mitigate adverse effects *in vivo*. An *in vitro* cell viability assay also demonstrated that squarticles with DA+rhein were well tolerated. In this study, we showed that lipid nanoparticles could sequester the toxicity of DA. The biocompatibility of squarticles to the cells contributed to the protection of cellular membrane from the damage by DA. These nanocarriers retained the fat-reducing activity of DA. The incorporation of rhein is important for the maintenance of the pharmacological activity of DA. Rhein is usually administered orally owing to its low aqueous solubility; however, it is difficult to achieve stable and effective concentrations in circulation.¹⁸ The inclusion of rhein in squarticles for injection could avoid this problem. Squarticle delivery via local administration may be a valuable strategy for maintaining fat-reducing effects with reduced toxicity.

The present study has some limitations. Intraperitoneal administration has been used to deliver the squarticles to treat obesity. However, this route is not commonly used to administer medications in humans. Further investigation is necessary to determine the fat-reducing effects of squarticles using other delivery routes for future clinical evaluation. For example, subcutaneous injections can be used to treat the adipose tissue. We verified the effects of squarticles in minimizing the toxicity of DA. This effect may be due to the avoidance of direct contact with the cell membrane. However, the mechanism by which lipid-based nanoparticles attenuate these side effects was not directly addressed in this study. The possible reasons for this need to be further examined to elucidate the underlying mechanisms. The antilipogenic activity of the combination of DA and rhein was partially compromised by nanoencapsulation. Formulation optimization of squarticles should be continued to enhance their therapeutic efficacy.

Conclusion

The development of anti-obesity drugs is an urgent requirement in modern medicine. Various adipocytolytic agents such as DA are used in dermatology and plastic surgery. However, significant adverse effects have reduced the clinical

applicability of adipocytolytic agents. Our data suggest that squarticles can be used as delivery carriers for DA. This nanosystem provides fat-reducing activity and reduces DA toxicity. DA induces adipocyte apoptosis and necrosis in squarticles to arrest fat accumulation. Rhein, with its distinct lipid-lowering mechanism compared to DA was incorporated into the nanoparticles to promote anti-adipogenic activity. The combination of DA and rhein in squarticles effectively inhibited the metabolic inflammation-related cytokines in adipocytes. In the obese rat model, the improvement in biochemical serum parameters was comparable between free compounds and squarticles. However, the adipokine inhibitory ability of the squarticles was lower than that of the free form. Nanoencapsulation reduced the in vivo toxicity of free DA+rhein, particularly its hepatotoxicity. Addition of rhein to DA-loaded squarticles mitigated HFD-induced adiposity and inflammation. This incorporation supplemented the partial loss of the fat-reducing activity of the nanoencapsulated DA. The low-dose nanoencapsulation of DA used in this study demonstrated the benefit of avoiding overt cell lysis to support homeostasis and prevent toxicity. Squarticles on antiadipogenic DA and rhein represent novel therapeutic approaches for treating obesity. Obesity is a chronic disease that usually needs long-term medication. The lipid-based nanoparticles with satisfied biocompatibility are favorable for anti-obesity treatment. Nevertheless, the safety of squarticles about the long-term use should be further examined in the future with the aim to confirm the applicability. For further examination of anti-obesity effect in clinical condition, the therapeutic activity of squarticles can be compared with that of conventional medication to explore the usefulness of this nanosystem.

Data Sharing Statement

Data are available on request from the authors.

Funding

This work was supported by National Science and Technology Council, Taiwan (MOST-110-2320-B-182-011-MY3) and Chang Gung Memorial Hospital (CMRPG3N0921).

Disclosure

The authors report no conflicts of interest in this work.

References

1. Kloock S, Ziegler CG, Dischinger U. Obesity and its comorbidities, current treatment options and future perspectives: challenging bariatric surgery? *Pharmacol Ther.* 2023;251:108549. doi:10.1016/j.pharmthera.2023.108549
2. Booth A, Magnuson A, Fouts J, Foster M. Adipose tissue, obesity and adipokines: role in cancer promotion. *Horm Mol Biol Clin Invest.* 2015;21:57–74.
3. Müller TD, Blüher M, Tschöp MH, DiMarchi RD. Anti-obesity drug discovery: advances and challenges. *Nat Rev Drug Discover.* 2022;21:201–223.
4. Li Q, Spalding KL. Profiling hypertrophic adipocytes in humans, from transcriptomics to diagnostics. *EBioMedicine.* 2022;81:104105. doi:10.1016/j.ebiom.2022.104105
5. Li H, Lee JH, Kim SY, et al. Phosphatidylcholine induces apoptosis of 3T3-L1 adipocytes. *J Biomed Sci.* 2011;18(1):91. doi:10.1186/1423-0127-18-91
6. Luk CT, Chan CK, Chiu F, et al. Dual role of caspase 8 in adipocyte apoptosis and metabolic inflammation. *Diabetes.* 2023;72(12):1751–1765. doi:10.2337/db22-1033
7. Liu M, Chesnut C, Lask G. Overview of Kybella (deoxycholic acid injection) as a fat resorption product for submental fat. *Facial Plast Surg.* 2019;35(3):274–277. doi:10.1055/s-0039-1688943
8. Watchmaker J, Callaghan III DJ, Dover JS. Deoxycholic acid in aesthetic medicine. *Adv Cosmet Surg.* 2020;3(1):77–87. doi:10.1016/j.yacs.2020.01.009
9. Muskat A, Pirtle M, Kost Y, McLellan BN, Shinoda K. The role of fat reducing agents on adipocyte death and adipose tissue inflammation. *Front Endocrinol.* 2022;13:841889. doi:10.3389/fendo.2022.841889
10. Zarbafian M, Karavan M, Greene R, Fabi SG. Efficacy and safety of ATX-101 as a treatment for submental fullness: a retrospective analysis of two aesthetic practices. *J Cosmet Dermatol.* 2020;19:1328–1332.
11. Pham CT, Lee A, Sung CT, Choi F, Juhasz M, Mesinkovska NA. Adverse events of injectable deoxycholic acid. *Dermatol Surg.* 2020;46(7):942–949. doi:10.1097/DSS.0000000000002318
12. Li J, Cha R, Luo H, Hao W, Zhang Y, Jiang X. Nanomaterials for the theranostics of obesity. *Biomaterials.* 2019;223:119474. doi:10.1016/j.biomaterials.2019.119474
13. Almeida H, Lobão P, Frigerio C, et al. Preparation, characterization and biocompatibility studies of thermoresponsive eyedrops based on the combination of nanostructured lipid carriers (NLC) and the polymer Pluronic F-127 for controlled delivery of ibuprofen. *Pharm Dev Technol.* 2017;22(3):336–349. doi:10.3109/10837450.2015.1125922

14. Ríos F, Fernández-Arteaga A, Fernández-Serrano M, Jurado E, Lechuga M. Silica micro- and nanoparticles reduce the toxicity of surfactant solutions. *J Hazard Mater*. 2018;353:436–443. doi:10.1016/j.jhazmat.2018.04.040
15. Sayed UFSM, Moshawih S, Goh HP, et al. Natural products as novel anti-obesity agents: insights into mechanisms of action and potential for therapeutic management. *Front Pharmacol*. 2023;14:1182937. doi:10.3389/fphar.2023.1182937
16. Zhang Y, Fan S, Hu N, et al. Rhein reduces fat weight in db/db mouse and prevents diet-induced obesity in C57Bl/6 mouse through the inhibition of PPAR γ signaling. *PPAR Res*. 2012;2012:374936. doi:10.1155/2012/374936
17. Fang JY, Huang TH, Chen WJ, Aljuffali IA, Hsu CY. Rhubarb hydroxyanthraquinones act as antiobesity agents to inhibit adipogenesis and enhance lipolysis. *Biomed Pharmacother*. 2022;146:112497. doi:10.1016/j.biopha.2021.112497
18. Li GM, Chen JR, Zhang HQ, et al. Update on pharmacological activities, security, and pharmacokinetics of rhein. *Evid Complement Altern Med*. 2021;2021:4582412.
19. Cheng L, Chen Q, Pi R, Chen J. A research update on the therapeutic potential of rhein and its derivatives. *Eur J Pharmacol*. 2021;899:173908. doi:10.1016/j.ejphar.2021.173908
20. Haider M, Abidin SM, Kamal L, Orive G. Nanostructured lipid carriers for delivery of chemotherapeutics: a review. *Pharmaceutics*. 2020;12(3):288. doi:10.3390/pharmaceutics12030288
21. Viegas C, Patrício AB, Prata JM, Nadhman A, Chintamaneni PK, Fonte P. Solid lipid nanoparticles vs. nanostructured lipid carriers: a comparative review. *Pharmaceutics*. 2023;15(6):1593. doi:10.3390/pharmaceutics15061593
22. Chen CH, Huang TH, Elzoghby A, Wang PW, Chang CW, Fang JY. Squarticles as the nanoantidotes to sequester the overdosed antidepressant for detoxification. *Int J Nanomed*. 2017;12:8071–8083. doi:10.2147/IJN.S143370
23. Aljuffali IA, Sung CT, Shen FM, Huang CT, Fang JY. Squarticles as a lipid nanocarrier for delivering diphencyprone and minoxidil to hair follicles and human dermal papilla cells. *AAPS J*. 2014;16(1):140–150. doi:10.1208/s12248-013-9550-y
24. Li H, Zhao X, Liu X, Tong Z, Lv Z. Rhodamine 800-labeled chitosan nanoparticles for intracellular tracking and cancer targeting. *Int J Pharm*. 2013;448:291–298.
25. Meador CK, Griffin AC. The oil red O stain for lipids. *Stain Technol*. 1961;36:317–321.
26. Riccardi C, Nicoletti I. Analysis of apoptosis by propidium iodide staining and flow cytometry. *Nat Protoc*. 2006;1(3):1458–1461. doi:10.1038/nprot.2006.238
27. Apostolou M, Assi S, Fatokun AA, Khan I. The effects of solid and liquid lipids on the physicochemical properties of nanostructured lipid carriers. *J Pharm Sci*. 2021;110(8):2859–2872. doi:10.1016/j.xphs.2021.04.012
28. Subramanian B, Siddik ZH, Nagoor NH. Optimization of nanostructured lipid carriers: understanding the types, designs, and parameters in the process of formulations. *J Nanopart Res*. 2020;22:141.
29. Akbari J, Saeedi M, Ahmadi F, et al. Solid lipid nanoparticles and nanostructured lipid carriers: a review of the methods of manufacture and routes of administration. *Pharm Dev Technol*. 2022;27(5):525–544. doi:10.1080/10837450.2022.2084554
30. Guru A, Issac PK, Velayutham M, Saraswathi NT, Arshad A, Arockiaraj J. Molecular mechanism of down-regulating adipogenic transcription factors in 3T3-L1 adipocyte cells by bioactive anti-adipogenic compounds. *Mol Biol Rep*. 2021;48(1):743–761. doi:10.1007/s11033-020-06036-8
31. Alalaiwe A, Fang JY, Lee HJ, Chiu CH, Hsu CY. The demethoxy derivatives of curcumin exhibit greater differentiation suppression in 3T3-L1 adipocytes than curcumin: a mechanistic study of adipogenesis and molecular docking. *Biomolecules*. 2021;11(7):1025. doi:10.3390/biom11071025
32. Tatewaki N, Konishi T, Nakajima Y, et al. Squalene inhibits ATM-dependent signaling in γ IR-induced DNA damage response through induction of Wip1 phosphatase. *PLoS One*. 2016;11(1):e0147570. doi:10.1371/journal.pone.0147570
33. Bidooki SH, Alejo T, Sánchez-Marco J, et al. Squalene loaded nanoparticles effectively protect hepatic AML12 cell lines against oxidative and endoplasmic reticulum stress in a TXNDC5-dependent way. *Antioxidants*. 2022;11(3):581. doi:10.3390/antiox11030581
34. Zhang W, Sheng T, Gu Z, Zhang Y. Strategies for browning agent delivery. *Pharm Res*. 2021;38(8):1327–1334. doi:10.1007/s11095-021-03081-1
35. Ahmad B, Serpell CJ, Fong IL, Wong EH. Molecular mechanisms of adipogenesis: the anti-adipogenic role of AMP-activated protein kinase. *Front Mol Biosci*. 2020;7:76.
36. Won TJ, Nam Y, Lee HS, et al. Injection of phosphatidylcholine and deoxycholic acid regulates gene expression of lipolysis-related factors, pro-inflammatory cytokines, and hormones on mouse fat tissue. *Food Chem Toxicol*. 2013;60:263–268. doi:10.1016/j.fct.2013.07.057
37. Batchuluun B, Pinkosky SL, Steinberg GR. Lipogenesis inhibitors: therapeutic opportunities and challenges. *Nat Rev Drug Discover*. 2022;21:283–305.
38. Teixeira C, Sousa AP, Santos I, et al. Enhanced 3T3-L1 differentiation into adipocytes by pioglitazone pharmacological activation of peroxisome proliferator activated receptor-gamma (PPAR- γ). *Biology*. 2022;11(6):806. doi:10.3390/biology11060806
39. Maximus PS, Al Achkar Z, Hamid PF, Hasnain SS, Peralta CA. Adipocytokines: are they the theory of everything? *Cytokine*. 2020;133:155144. doi:10.1016/j.cyto.2020.155144
40. Ge H, Tang H, Liang Y, et al. Rhein attenuates inflammation through inhibition of NF-kappaB and NALP3 inflammasome in vivo and in vitro. *Drug Des Dev Ther*. 2017;11:1663–1671. doi:10.2147/DDDT.S133069
41. Lin N, Song X, Chen B, et al. Leptin is upregulated in epididymitis and promotes apoptosis and IL-1 β production in epididymal epithelial cells by activating the NLRP3 inflammasome. *Int Immunopharmacol*. 2020;88:106901. doi:10.1016/j.intimp.2020.106901
42. Wollina U, Goldman A. ATX-101 for reduction of submental fat. *Expert Opin Pharmacother*. 2015;16(5):755–762. doi:10.1517/14656566.2015.1019465
43. Monji A, Zhang Y, Kumar GVN, et al. A cycle of inflammatory adipocyte death and regeneration in murine adipose tissue. *Diabetes*. 2022;71(3):412–423. doi:10.2337/db20-1306
44. Yuan JT, Shafiq F. Safety and efficacy of deoxycholic acid for reduction of upper inner thigh fat. *J Drugs Dermatol*. 2022;21:66–70. doi:10.36849/JDD.5919
45. Hildebrandt X, Ibrahim M, Peltzer N. Cell death and inflammation during obesity: “know my methods, WAT(son)”. *Cell Death Differ*. 2023;30(2):279–292. doi:10.1038/s41418-022-01062-4
46. Bu S, Xiong A, Yang Z, et al. Bilobalide induces apoptosis in 3T3-L1 mature adipocytes through ROS-mediated mitochondria pathway. *Molecules*. 2023;28(17):6410. doi:10.3390/molecules28176410
47. You L, Dong X, Yin X, et al. Rhein induces cell death in hepaRG cells through cell cycle arrest and apoptotic pathway. *Int J Mol Sci*. 2018;19(4):1060. doi:10.3390/ijms19041060

48. Cunha KS, Lima F, Cardoso RM. Efficacy and safety of injectable deoxycholic acid for submental fat reduction: a systematic review and meta-analysis of randomized controlled trials. *Expert Opin Clin Pharmacol.* 2021;14(3):383–397. doi:10.1080/17512433.2021.1884070
49. Sushnitha M, Evangelopoulos M, Tasciotti E, Taraballi F. Cell membrane-based biomimetic nanoparticles and the immune system: immunomodulatory interactions to therapeutic applications. *Front Bioeng Biotechnol.* 2020;8:627. doi:10.3389/fbioe.2020.00627
50. Saltiel AR, Olefsky JM. Inflammatory mechanisms linking obesity and metabolic disease. *J Clin Invest.* 2017;127(1):1–4. doi:10.1172/JCI92035
51. de Queiroz JLC, Medeiros I, MSR L, et al. Efficacy of carotenoid-loaded gelatin nanoparticles in reducing plasma cytokines and adipocyte hypertrophy in Wistar rats. *Int J Mol Sci.* 2023;24(13):10657. doi:10.3390/ijms241310657
52. Picó C, Palou M, Pomar CA, Rodríguez AM, Palou A. Leptin as a key regulator of the adipose organ. *Rev Endocr Metab Disord.* 2022;23(1):13–30. doi:10.1007/s11154-021-09687-5
53. Al-Mansoori L, Al-Jaber H, Prince MS, Elrayess MA. Role of inflammatory cytokines, growth factors and adipokines in adipogenesis and insulin resistance. *Inflammation.* 2022;45(1):31–44. doi:10.1007/s10753-021-01559-z
54. Hong J, Kim YH. Fatty liver/adipose tissue dual-targeting nanoparticles with heme oxygenase-1 inducer for amelioration of obesity, obesity-induced type 2 diabetes, and steatohepatitis. *Adv Sci.* 2022;9(33):2203286. doi:10.1002/advs.202203286
55. Gao Y, Chen X, Fang L, et al. Rhein exerts pro- and anti-inflammatory actions by targeting IKK β inhibition in LPS-activated macrophages. *Free Radic Biol Med.* 2014;72:104–112. doi:10.1016/j.freeradbiomed.2014.04.001
56. Zhang K, Jiao XF, Li JX, Wang XW. Rhein inhibits lipopolysaccharide-induced intestinal injury during sepsis by blocking the toll-like receptor 4 nuclear factor- κ B pathway. *Mol Med Rep.* 2015;12(3):4415–4421. doi:10.3892/mmr.2015.3925
57. Tu Y, Gu L, Chen D, et al. Rhein inhibits autophagy in rat renal tubular cells by regulation of AMPK/mTOR signaling. *Sci Rep.* 2017;7(1):43790. doi:10.1038/srep43790
58. Wallace M, Metallo CM. Tracing insights into de novo lipogenesis in liver and adipose tissues. *Semin Cell Dev Biol.* 2020;108:65–71. doi:10.1016/j.semedb.2020.02.012
59. Alves-Bezerra M, Cohen DE. Triglyceride metabolism in the liver. *Compr Physiol.* 2018;8:1–22.
60. Duncan D, Rubin JP, Golitz L, et al. Refinement of technique in injection lipolysis based on scientific studies and clinical evaluation. *Clin Plast Surg.* 2009;36(2):195–209. doi:10.1016/j.cps.2008.11.001
61. Yang D, Huang WY, Li YQ, et al. Acute and subchronic toxicity studies of rhein in immature and d-galactose-induced aged mice and its potential hepatotoxicity mechanisms. *Drug Chem Toxicol.* 2022;45(3):1119–1130. doi:10.1080/01480545.2020.1809670
62. Ryabova YV, Minigalieva IA, Sutunkova MP, et al. Toxic kidney damage in rats following subchronic intraperitoneal exposure to element oxide nanoparticles. *Toxics.* 2023;11(9):791. doi:10.3390/toxics11090791

International Journal of Nanomedicine

Dovepress

Publish your work in this journal

The International Journal of Nanomedicine is an international, peer-reviewed journal focusing on the application of nanotechnology in diagnostics, therapeutics, and drug delivery systems throughout the biomedical field. This journal is indexed on PubMed Central, MedLine, CAS, SciSearch[®], Current Contents[®]/Clinical Medicine, Journal Citation Reports/Science Edition, EMBase, Scopus and the Elsevier Bibliographic databases. The manuscript management system is completely online and includes a very quick and fair peer-review system, which is all easy to use. Visit <http://www.dovepress.com/testimonials.php> to read real quotes from published authors.

Submit your manuscript here: <https://www.dovepress.com/international-journal-of-nanomedicine-journal>